JACS
JOURNAL OF THE AMERICAN CHEMICAL SOCIETY
Article
pubs.acs.org/JACS

Why the Mechanisms of Digermyne and Distannyne Reactions with H_2 Differ So Greatly

LiLi Zhao,[†] Fang Huang,[†] Gang Lu,[†] Zhi-Xiang Wang,*[,†] and Paul von Ragué Schleyer*[,‡]

[†]College of Chemistry and Chemical Engineering, Graduate University of the Chinese Academy of Sciences, Beijing 100049, P. R. China

[‡]Department of Chemistry, University of Georgia, Athens, Georgia 30602, United States

Supporting Information

ABSTRACT: Despite their formal relationship to alkynes, Ar′GeGeAr′, Ar′SnSnAr′, and Ar*SnSnAr* [Ar′ = 2,6-(2,6-iPr$_2$C$_6$H$_3$)$_2$C$_6$H$_3$; Ar* = 2,6-(2,4,6-iPr$_3$C$_6$H$_2$)$_2$-3,5-iPr$_2$C$_6$H] exhibit high reactivity toward H_2, quite unlike acetylenes. Remarkably, the products are totally different. Ar′GeGeAr′ can react with 1−3 equiv of H_2 to give mixtures of Ar′HGeGeHAr′, Ar′H$_2$GeGeH$_2$Ar′, and Ar′GeH$_3$. In contrast, Ar′SnSnAr′ and Ar*SnSnAr* react with only 1 equiv of H_2 but give different types of products, Ar′Sn(μ-H)$_2$SnAr′ and Ar*SnSnH$_2$Ar*, respectively. In this work, this disparate behavior toward H_2 has been elucidated by TPSSTPSS DFT computations of the detailed reaction mechanisms, which provide insight into the different pathways involved. Ar′GeGeAr′ reacts with H_2 via three sequential steps: H_2 addition to Ar′GeGeAr′ to give singly H-bridged Ar′Ge(μ-H)GeHAr′; isomerization of the latter to the more reactive Ge(II) hydride Ar′GeGeH$_2$Ar′; and finally, addition of another H_2 to the hydride, either at a single Ge site, giving Ar′H$_2$GeGeH$_2$Ar′, or at a Ge−Ge joint site, affording Ar′GeH$_3$ + Ar′HGe:. Alternatively, Ar′Ge(μ-H)GeHAr′ also can isomerize into the kinetically stable Ar′HGeGeHAr′, which cannot react with H_2 directly but can be transformed to the reactive Ar′GeGeH$_2$Ar′. The activation of H_2 by Ar′SnSnAr′ is similar to that by Ar′GeGeAr′. The resulting singly H-bridged Ar′Sn(μ-H)SnHAr′ then isomerizes into Ar′HSnSnHAr′. The subsequent facile dissociation of the latter gives two Ar′HSn: species, which then reassemble into the experimental product Ar′Sn(μ-H)$_2$SnAr′. The reaction of Ar*SnSnAr* with H_2 forms in the kinetically and thermodynamically more stable Ar*SnSnH$_2$Ar* product rather than Ar*Sn(μ-H)$_2$SnAr*. The computed mechanisms successfully rationalize all of the known experimental differences among these reactions and yield the following insights into the behavior of the Ge and Sn species: (I) The active sites of Ar′EEAr′ (E = Ge, Sn) involve both E atoms, and the products with H_2 are the singly H-bridged Ar′E(μ-H)EHAr′ species rather than Ar′HEEHAr′ or Ar′EEH$_2$Ar′. (II) The heavier alkene congeners Ar′HEEHAr′ (E = Ge, Sn) cannot activate H_2 directly. Instead, Ar′HGeGeHAr′ must first isomerize into the more reactive Ar′GeGeH$_2$Ar′. Interestingly, the subsequent H_2 activation by Ar′GeGeH$_2$Ar′ can take place on either a single Ge site or a joint Ge−Ge site, but Ar′SnSnH$_2$Ar′ is not reactive toward H_2. The higher reactivity of Ar′GeGeH$_2$Ar′ in comparison with Ar′SnSnH$_2$Ar′ is due to the tendency of group 14 elements lower in the periodic table to have more stable lone pairs (i.e., the inert pair effect) and is responsible for the differences between the reactions of Ar′EEAr′ (E = Ge, Sn) with H_2. Similarly, the carbene-like Ar′HGe: is more reactive toward H_2 than is Ar′HSn:. (III) The doubly H-bridged Ar′E(μ-H)$_2$EAr′ (E = Ge, Sn) species are not reactive toward H_2.

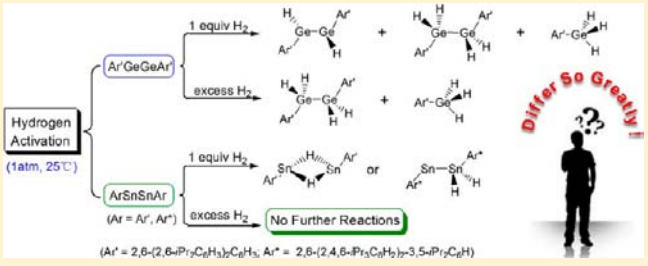

1. INTRODUCTION

Dihydrogen activation not only is a crucial chemical process (e.g., its involvement in catalytic hydrogenation)[1] but also enriches our understanding of the reactivity of unsaturated compounds.[2] The mechanisms whereby many transition metal (TM) complexes cleave dihydrogen readily are well-documented.[2,3] In contrast, hydrogen activation by main-group compounds *under mild conditions* was unknown until 2005, when Power and co-workers discovered that, unlike acetylenes, their heavier germanium congeners [e.g., Ar′GeGeAr′, Ar′ = 2,6-(2,6-iPr$_2$C$_6$H$_3$)$_2$C$_6$H$_3$] can react with H_2 at 25 °C and 1 atm pressure (eq 1).[4] Earlier examples of TM-free hydrogen activation involved transient main-group species generated by extreme methods (e.g., laser ablation)[5] and TM-free hydrogenation under forcing conditions (135 bar and 210 °C).[6] Noteworthy metal-free hydrogen activation systems were subsequently developed. Stephan's 2006 discovery that phosphonium borate (C$_6$H$_2$Me$_3$)$_2$P(C$_6$F$_4$)B(C$_6$F$_5$)$_2$ can activate H_2 reversibly[7] opened the area of frustrated Lewis pair (FLP) chemistry,[8] which has been applied to the realization of metal-free catalytic hydrogenation and the activation of other small molecules. Inspired by these experimental studies[8] as well as the detailed mechanism unveiled by Pápai and co-workers[9] and Guo and Li,[10] we proposed strategies to design metal-free molecules with active sites for dihydrogen and methane

Received: January 5, 2012
Published: April 23, 2012

   dx.doi.org/10.1021/ja300111q | J. Am. Chem. Soc. 2012, 134, 8856−8868

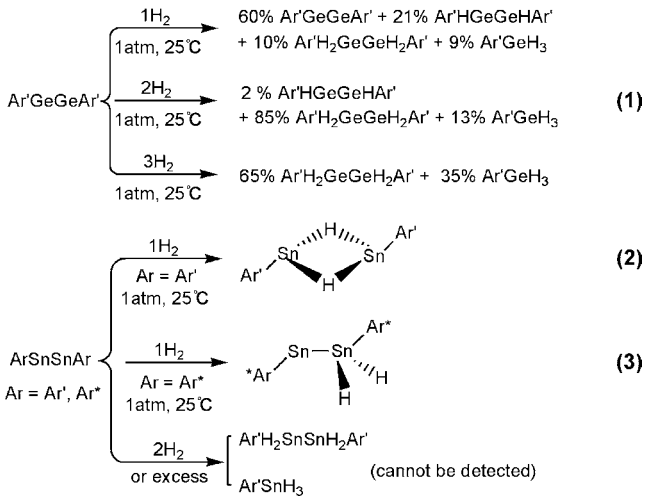

activations[11] and for imine and ketone hydrogenations.[12] These active-site designs anticipated features similar to those in compounds synthesized later by Tamm and co-workers,[13] the Lammertsma and Uhl groups,[14a] and the Slootweg and Lammertsma groups.[14b] Bertrand discovered in 2007 that stable (alkyl)(amino)carbenes can activate hydrogen just like TM complexes.[15] Radom's elegant investigations included quantum-chemical calculations to help understand TM-free H_2 activation/hydrogenation[16] and the design of TM-free catalysts for the transformation of CO_2 into methanol.[17]

The chemistry of the heavier alkyne congeners (i.e., REER, E = Si, Ge, Sn, Pb; R = aryl, alkyl, silyl) has been developed significantly in the past decades.[18−20] The heavier alkyne analogues have not only been synthesized but also been found to exhibit novel reactivities toward both saturated (e.g., H_2,[4,21] H_2O,[20g] and CH_3OH[20g]) and unsaturated molecules (e.g., olefins,[20e−k] R_2NO,[20c] CO,[20r] O_2,[20m] and nitriles[19k]). Heavier compounds of group 13 elements also were found to react with H_2, NH_3, and olefins.[22] Most recently, the Jones and Frenking groups synthesized LGeGeL [L = (Me_3Si)(4-Me-2,6-{C(H)-Ph_2}$_2C_6H_2$)N] and found that it reacted with H_2.[23] Although the alkyne congeners of Si and Pb have been prepared,[19] their reactions with H_2 have not been reported.

The present study focuses on the differences in the reactivities of the digermyne Ar′GeGeAr′ and the distannynes Ar′SnSnAr′ and Ar*SnSnAr* [Ar* = 2,6-(2,4,6-iPr$_3C_6H_2$)$_2$-3,5-iPr$_2C_6H$] toward H_2, as summarized in eqs 1−3. While the digermyne can react with 1−3 equiv of H_2, giving mixtures of the products[4] Ar′HGeGeHAr′, Ar′H_2GeGeH_2Ar′, and Ar′GeH_3 (eq 1), the distannynes react only with 1 equiv of H_2 under ambient conditions to give completely different products, doubly H-bridged Ar′Sn(μ-H)$_2$SnAr′ (eq 2) and the Sn(II) hydride Ar*SnSnH_2Ar* (eq 3), respectively.[21] Even when the distannynes were exposed to an excess H_2 atmosphere, the Sn analogues of Ar′HGeGeHAr′, Ar′H_2GeGeH_2Ar′, and Ar′GeH_3 could not be obtained.[21]

The syntheses of these novel heavier alkyne congeners has elicited extensive computational investigations of the nature of their chemical bonding,[24] but only a limited number of computational studies on their reactivity have been reported. To our knowledge, only Nagase, Power, and co-workers have investigated the reactions of the germylene Ar′$_2$Ge: and the stannylene Ar′$_2$Sn: with H_2 and NH_3 computationally, in conjunction with their experimental studies.[25] Unlike the case of alkynes, the molecular orbital (MO) interactions between the alkyne congeners and H_2 are symmetry-allowed.[18a,b] However, the mechanisms of the reactions in eqs 1−3 remain elusive. This has stimulated us to carry out detailed mechanistic studies to understand why the reactivities of the Ge and Sn alkyne congeners toward H_2 are so different. Unveiling the root causes could help in the further development of the chemistry of group 14 elements.

2. COMPUTATIONAL DETAILS

All of the computations used the Gaussian 03 program.[26] We first established a practicable density functional theory (DFT) level for describing larger systems with 136−210 atoms by using $CH_3SnSnCH_3$ as a simplified model. By comparing the performance of various combinations of DFT functionals (TPSSTPSS,[27] B3PW91,[28] B3LYP,[29] and M05-2X[30]) and basis sets (SDD,[31] LANL2DZ,[32] aug-cc-pVDZ-pp,[33] aug-cc-pVTZ-pp,[33] def2-svp,[34] and def2-tzvp[34] for Sn and 6-31G*[35] for C and H) with previously reported second-order Møller−Plesset perturbation theory (MP2) results[24i] (for details, see section SI1 in the Supporting Information), we ascertained that the TPSSTPSS/BSI method outperforms the others (BSI denotes the combination of the def2-tzvp basis set for Sn and the 6-31G* basis set for C and H). The accuracy of the TPSSTPSS/BSI results were established further by single-point ONIOM[36] computations at the CCSD(T)/BSI:TPSSTPSS/BSI//TPSSTPSS/BSI level for the reaction of Ar′SnSnAr′ with H_2 to give doubly H-bridged Ar′Sn(μ-H)$_2$SnAr′. In the ONIOM calculations, the two Sn atoms, the C and H atoms of the two central aryl rings directly bonded to the Sn atoms, and the two H atoms of H_2 were described at the CCSD(T)/BSI level and other C and H atoms at the TPSSTPSS/BSI level. The predicted exothermicity (ΔH = −14.6 kcal/mol) at the TPSSTPSS/BSI level is close to the −15.8 kcal/mol given by the ONIOM computations (section SI2). Therefore, TPSSTPSS/BSI was used throughout this study.

The geometries corresponding to the (unsimplified) experimental compounds were fully optimized at the TPSSTPSS/BSI level in the gas phase (the def2-tzvp basis set was used for Ge also). Harmonic vibrational frequency analyses were used to characterize the stationary points as transition states or minima. Using PhGeGePh as a model, we also conducted TPSSTPSS/BSI intrinsic reaction coordinate (IRC) calculations (precluded by the large size of the experimental systems) to verify the critical reaction steps involved in our proposed mechanisms. As the simplified heavier alkyne models (CH_3EECH_3, E = Ge, Sn) were reported to have some diradical character,[24k] we verified the stability of the DFT wave functions of the multiply bonded Ar′GeGeAr′ and Ar′SnSnAr′ species as well as the hydrogen-activation transition states. However, the DFT wave functions of their singly bonded forms were unstable. The optimized geometries of Ar′GeGeAr′ and Ar′SnSnAr′ agreed well with their X-ray crystal structures (Figure 1). Solvent effects were simulated using integral equation formalism polarizable continuum solvent model (IEFPCM)[37] single-point calculations carried out on the TPSSTPSS/BSI gas-phase geometries at the TPSSTPSS/BSII level with the universal force field (UFF)[38] atomic radii (BSII denotes the use of the def2-tzvp basis set for all atoms). The heptane parameters available in Gaussian were used to evaluate the reaction shown in eq 1 (hexane was employed experimentally but was not available in Gaussian 03), and toluene parameters were used for the reactions in eqs 2 and 3. The TPSSTPSS/BSI harmonic vibrational frequencies were used for thermal and entropic corrections at 298.15 K and 1 atm. Gibbs free energies are discussed, unless otherwise specified; enthalpies also are given for reference in the related schemes and figures.

3. RESULTS AND DISCUSSION

The goal of the present study is to elucidate the detailed mechanisms of the reactions of H_2 with the digermyne Ar′GeGeAr′ and the distannynes Ar′SnSnAr′ and Ar*SnSnAr* in order to understand the differences in behavior summarized by eqs 1−3.

dx.doi.org/10.1021/ja300111q | J. Am. Chem. Soc. 2012, 134, 8856−8868

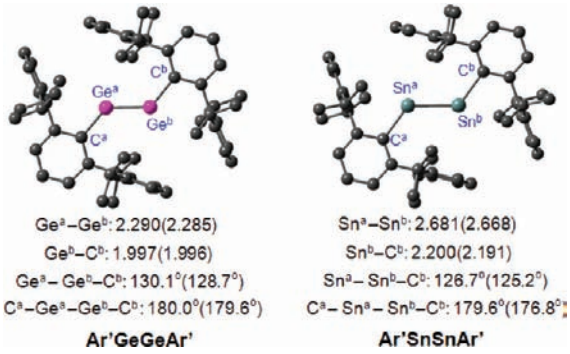

Figure 1. Optimized structures of Ar′GeGeAr′ and Ar′SnSnAr′. Key bond distances, bond angles, and dihedral angles are given in angstroms and degrees, respectively. Experimental values from the X-ray structures of Ar′GeGeAr′[20a] and Ar′SnSnAr′[20b] are given in parentheses. H atoms have been omitted for clarity. Color code: C, black; Ge, purple; Sn, dark-gray.

3.1. Mechanism of the Reaction of Ar′GeGeAr′ with H_2 (eq 1). Power and co-workers demonstrated that Ar′GeGeAr′ reacts with H_2 under ambient conditions (25 °C and 1 atm) to give the products shown in eq 1.[4] On the basis of the isolated products, they postulated a reaction sequence for the reaction (Scheme 1A).[4] H_2 could add to Ar′GeGeAr′ to give the digermene Ar′HGeGeHAr′, which could react with another H_2 to afford the digermane Ar′H_2GeGeH_2Ar′. Alternatively, Ar′HGeGeHAr′ could also equilibrate with two Ar′HGe: as well as with the doubly H-bridged Ar′Ge(μ-H)$_2$GeAr′. The latter [either Ar′HGe: or Ar′Ge(μ-H)$_2$GeAr′] could react further with H_2 to generate the primary germane Ar′GeH_3. A slightly different reaction sequence (Scheme 1B) was suggested recently.[18a] The reaction of dihydrogen with Ar′GeGeAr′ might take place on a single Ge site to give the asymmetric Ge(II) hydride Ar′GeGeH_2Ar′, which then could isomerize to Ar′HGeGeHAr′. The isomer could either react further with H_2 to give Ar′H_2GeGeH_2Ar′ or dissociate into Ar′HGe:, which could then react further with H_2 to give Ar′GeH_3.

The energy diagram shown in Scheme 2 describes the detailed reaction mechanism predicted by our computations. The optimized structures of key stationary points in Scheme 2 are displayed in Figure 2 (those not shown are given in section SI3).

Our computed energies agree with Power and co-workers' experimental observations that Ar′GeGeAr′ can activate H_2 under mild conditions.[4] The free energy barrier (**TS1**, 18.4 kcal/mol) is low enough to be experimentally accessible, and product (**IM1**) formation is exergonic by 10.5 kcal/mol. The enthalpy barrier (8.2 kcal/mol) is comparable to other barriers for H_2 activation under mild conditions, including 8−10 kcal/mol for TM hydrogenation catalyst models,[39] 10.4 kcal/mol for the typical (tBu)$_3$P/B(C_6F_5)$_3$ FLP,[9] ca. 22 kcal/mol for the (tBu)$_2$PB(C_6F_5)$_2$ FLP,[40,12a] and 22−26 kcal/mol for mono-(amino)carbene models.[15] The dihydrogen H−H bond and the Ge−Ge bond in **TS1** are stretched to 0.953 and 2.601 Å from 0.741 Å in H_2 and 2.290 Å in Ar′GeGeAr′, respectively. The two nascent Ge−H bonds (1.722 and 2.389 Å; see Figure 2) form concurrently. Thus, **TS1** involves a Ge−Ge bond rather than a single Ge atom site and leads to singly H-bridged Ar′Ge(μ-H)GeHAr′ (**IM1**). The validity of the **TS1** to **IM1** connection was verified by the following observations: The vector of the vibrational mode of the **TS1** imaginary frequency describes the incipient bonding of H^a with Ge^a as well as the movement of H^b toward Ge^b (section SI4). Extensive searches for H_2-activation transition states having a single Ge atom as the active site led either to **TS1** or the separated reactants (Ar′GeGeAr′ + H_2). Optimizations using initial geometries slightly displaced from **TS1** led to **IM1**. In addition, IRC calculations on the PhGeGePh model led to the **IM1** analogue (section SI5). This study indicates that H_2 activation by Ar′GeGeAr′ does not lead *directly* to either the digermene Ar′HGeGeHAr′ in Scheme 1A or the asymmetric Ge(II) hydride Ar′GeGeH_2Ar′ in Scheme 1B.

The digermene Ar′HGeGeHAr′ in Scheme 1 was postulated to be the key intermediate leading to the experimentally observed products.[4,18a] We found that the isomerization of **IM1** into the 6.7 kcal/mol more stable *trans*-Ar′HGeGeHAr′ proceeds by crossing a 6.5 kcal/mol barrier (**TS2**) and is exergonic by 17.2 kcal/mol relative to Ar′GeGeAr′ + H_2. The Ge−Ge bond in Ar′HGeGeHAr′ (2.332 Å) is elongated relative to that in Ar′GeGeAr′ (2.290 Å), but the C^a−Ge^a−Ge^b−C^b dihedral angle of 180.0° is retained. However, the reaction barrier for H_2 addition to Ar′HGeGeHAr′ to give

Scheme 1. Previously Proposed Reaction Sequences for the Reaction Shown in eq 1;[4,18a] The Molecules in the Boxes Are the Experimentally Isolated Products

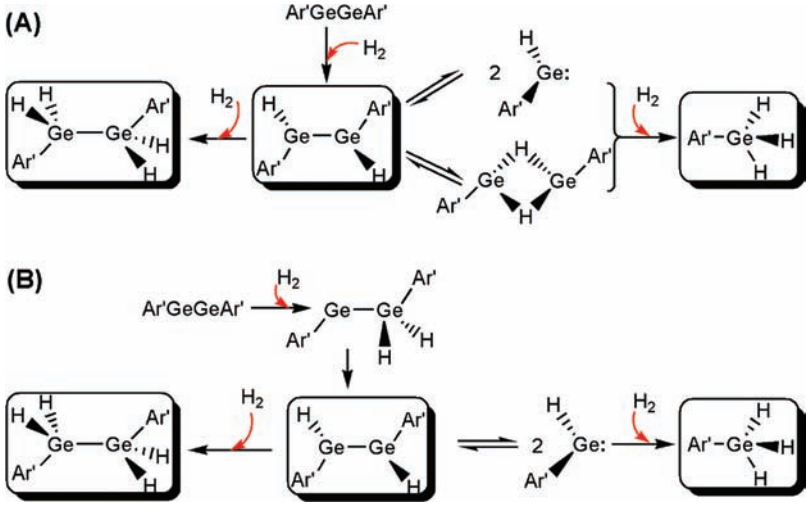

dx.doi.org/10.1021/ja300111q | J. Am. Chem. Soc. 2012, 134, 8856−8868

Scheme 2. Free Energy Profile for the Reaction of Ar′GeGeAr′ with H_2 (eq 1)[a]

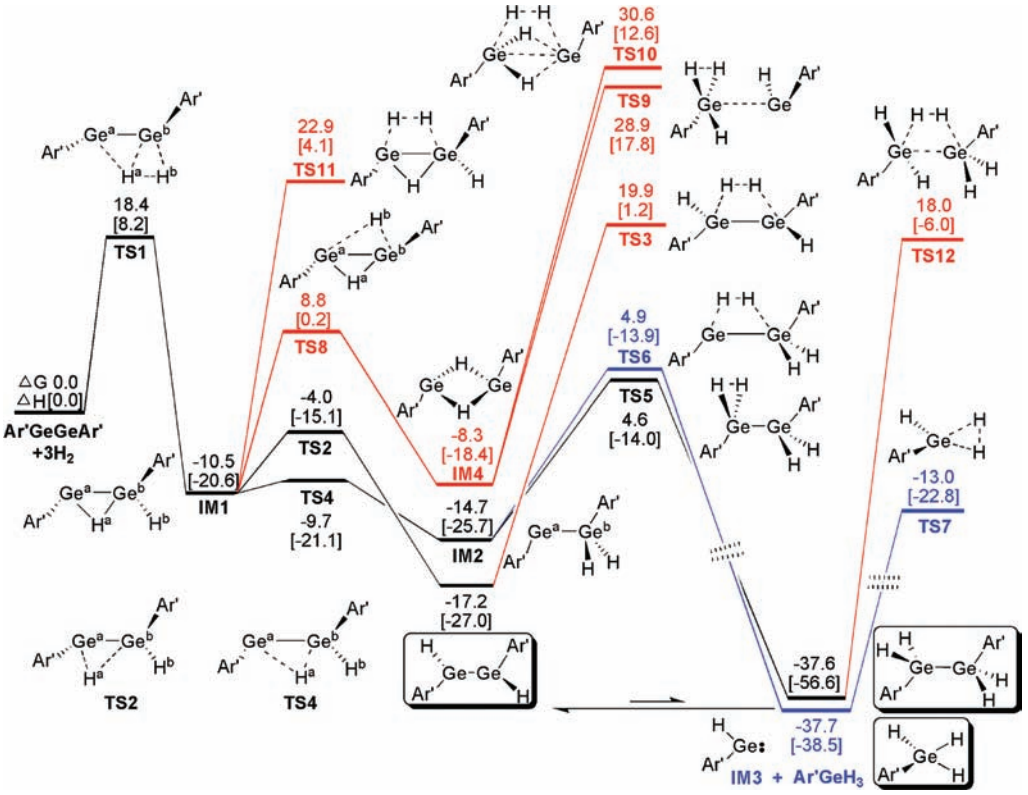

[a]Values shown are relative free energies, with enthalpies given in square brackets (all in kcal/mol). The pathways leading to the experimental products (enclosed in the boxes) are shown in black or blue. Other less favorable pathways are shown in red.

$Ar'H_2GeGeH_2Ar'$ (**TS3**, 37.1 kcal/mol relative to Ar′HGeGeHAr′ + H_2) is too high considering the mild experimental conditions. The isomerization from **IM1** to the *trans*-Ar′HGeGeHAr′ via **TS2** was verified by IRC calculations on the PhGeGePh model (section SI6). The cis isomer of Ar′HGeGeHAr′ (see Figure 2) is 11.6 kcal/mol higher in energy than the trans isomer because of the steric effect of the bulky Ar′ substituents.

A more favorable pathway leading to the digermane product $Ar'H_2GeGeH_2Ar'$ is shown in Scheme 2. After passing through a very low barrier (**TS4**, 0.8 kcal/mol), the bridging H^a in **IM1** can migrate to Ge^b easily, giving the asymmetric Ge(II) hydride $Ar'GeGeH_2Ar'$ (**IM2**). Notably, while **IM2** was not directly observed experimentally in the reaction of Ar′GeGeAr′ with H_2,[4] its trapping product with PMe_3, the $Ar'(PMe_3)GeGeH_2Ar'$ adduct, was identified by X-ray diffraction.[41] The elongated Ge^a–H^a bond (2.297 Å) and shortened H^a–Ge^b bond (1.621 Å) in **TS4** and the IRC calculations on the PhGeGePh model (section SI7) confirmed this migration step. The step from **IM1** to **IM2** is exergonic by 4.2 kcal/mol. Thus, the isomerization of **IM1** to **IM2** ($Ar'GeGeH_2Ar'$) is 5.7 kcal/mol more favorable kinetically but 2.5 kcal/mol less favorable thermodynamically than the isomerization to Ar′HGeGeHAr′. We confirmed the ground state of the carbene analogue **IM2** to be a singlet that is 15.6 kcal/mol lower in energy than the triplet. The isomerization from **IM1** to **IM2** allows the reaction with another H_2. Interestingly, the activation of H_2 by **IM2** ($Ar'Ge^aGe^bH_2Ar'$) can take place at either the single Ge^a site via transition state **TS5** (the black path) or the Ge^a–Ge^b site via **TS6** (the blue path). The black path crosses a 19.3 kcal/mol barrier (**TS5**) to give the observed product $Ar'H_2GeGeH_2Ar'$ and is highly exergonic (37.6 kcal/mol) relative to Ar′GeGeAr′ + $2H_2$. The blue path is exergonic by 37.7 kcal/mol and overcomes a slightly higher barrier (**TS6**, 19.6 kcal/mol) to give the intermediate Ar′HGe: (**IM3**) and the observed $Ar'GeH_3$ product. The complex between **IM3** and $Ar'GeH_3$ (shown in section SI8 but not in Scheme 2) was optimized and found to be only an unstable minimum, 19.8 kcal/mol higher in energy than **IM3** + $Ar'GeH_3$. The optimized structures of **TS5** and **TS6** (Figure 2) differentiate the two H_2 activation modes of $Ar'GeGeH_2Ar'$, and IRC calculations on the PhGeGePh model verified the two processes (section SI8). The **IM3** intermediate, Ar′HGe:, is a carbene analogue that we confirmed to have a singlet ground state (the triplet energy is 25.3 kcal/mol higher). Two reaction channels are possible for the further reactions of **IM3** (Ar′HGe:). (I) **IM3** could first dimerize to give Ar′HGeGeHAr′, which would then follow the **TS2** → **IM1** → **TS4** → **IM2** → **TS5**/**TS6** pathway to reach the more stable $Ar'H_2GeGeH_2Ar'$ or $Ar'GeH_3$ + **IM3** product set (Scheme 2). The dimerization is barrierless (see section SI9 for details). In terms of enthalpy and free energy, the dimerization is exergonic by 20.0 and 2.3 kcal/mol, respectively. It should be noted that the exergonicity in free energy would be greater (11.2 kcal/mol) after correction for the overestimation of the entropy contribution given by the ideal gas phase model (see Table 1 below for details). Another possible dimerization to give $Ar'Ge(\mu\text{-}H)_2GeAr'$ (**IM4**) would not be competitive because **IM4** is 8.9 kcal/mol higher than Ar′HGeGeHAr′. (II) Alternatively, the **IM3** species could activate H_2 by overcoming a 24.7 [i.e., −13.0 − (−37.7)] kcal/mol barrier (**TS7**) to give $Ar'GeH_3$ that is 22.8 kcal/mol more stable than **IM3** + H_2 (not shown in Scheme 2). Comparison of the energies of the two

dx.doi.org/10.1021/ja300111q | J. Am. Chem. Soc. 2012, 134, 8856−8868

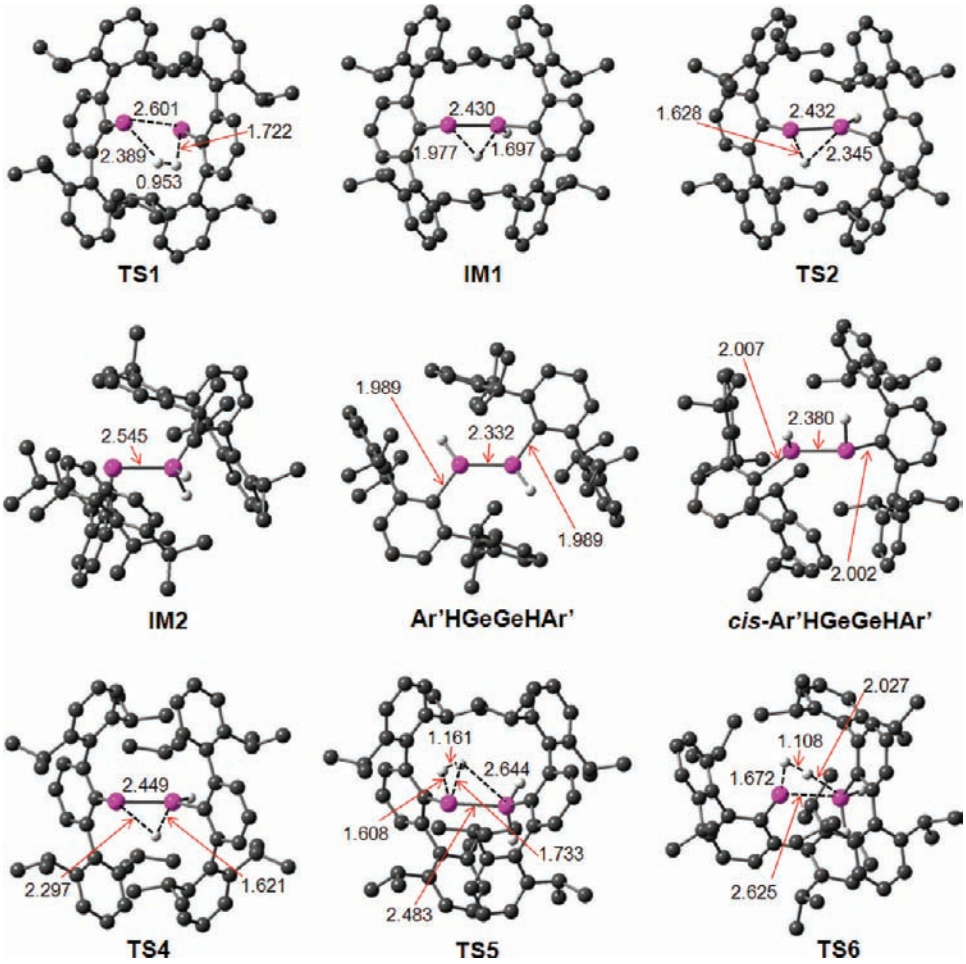

Figure 2. Optimized structures of some of the stationary points in Scheme 2, along with the key bond distances in Å. Trivial H atoms have been omitted for clarity. Color code: C, black; H, white; Ge, purple.

channels shows the former channel to be energetically more favorable, as the association of **IM3** to give Ar′HGeGeHAr′ is spontaneous and exergonic and the largest barriers in the channel (ca. 22.0 kcal/mol measured from Ar′HGeGeHAr′ to **TS5**/**TS6** along the Ar′HGeGeHAr′ → **TS2** → **IM1** → **TS4** → **IM2** → **TS5**/**TS6** → $Ar'H_2GeGeH_2Ar'$/**IM3** + $Ar'GeH_3$ pathway) is lower than the barrier for H_2 activation by **IM3** (24.7 kcal/mol).

As illustrated in Scheme 1, it was speculated that $Ar'GeH_3$ might result from the reaction of H_2 with either Ar′HGe: (**IM3**) or the doubly H-bridged $Ar'Ge(\mu\text{-}H)_2GeAr'$ (**IM4**),[4] which could be obtained from the dissociation or rearrangement of Ar′HGeGeHAr′. For the pathway via dissociation, the total energy cost is 27.0 kcal/mol (the sum of 2.3 kcal/mol for the Ar′HGeGeHAr′ → 2Ar′HGe: dissociation and 24.7 kcal/mol for the Ar′HGe: + H_2 → **TS7** → $Ar'GeH_3$ activation process), which is substantially higher than the barrier of 22.1 kcal/mol along the Ar′HGeGeHAr′ → **TS2** → **IM1** → **TS4** → **IM2** → **TS6** → **IM3** + $Ar'GeH_3$ pathway. For the pathway via **IM4**, as shown in Scheme 2, the **IM1** → **TS8** → **IM4** process to form **IM4** is kinetically and thermodynamically less favorable than the process to form **IM2** and Ar′HGeGeHAr′. Moreover, **IM4** cannot react with H_2 because of the higher barriers of 37.2 (**TS9**) and 38.9 kcal/mol (**TS10**) measured from **IM4** + H_2. Therefore, $Ar'Ge(\mu\text{-}H)_2GeAr'$ is not a likely intermediate leading to $Ar'GeH_3$.

In addition to all of the pathways considered above, we examined other possibilities (also colored in red in Scheme 2). These include direct H_2 activation by the singly H-bridged **IM1** via **TS11** and the direct addition of H_2 to $Ar'H_2GeGeH_2Ar'$ via **TS12** leading to 2 equiv of $Ar'GeH_3$. These possibilities are safely eliminated by the TS energies given in Scheme 2. The 55.6 [i.e., (18.0 − (−37.6)] kcal/mol barrier for its hydrogenolysis into two $Ar'GeH_3$ molecules (**TS12**) explains why $Ar'H_2GeGeH_2Ar'$ persists even in an atmosphere containing excess H_2.

The computed mechanism (Scheme 2) explains the production of the experimental products (enclosed in boxes). Although Ar′HGeGeHAr′ is the most stable isomer for $Ge_2H_2Ar'_2$, it can isomerize slightly endergonically into the more reactive **IM2** along the Ar′HGeGeHAr′ → **TS2** → **IM1** → **TS4** → **IM2** pathway. The viability of this route is supported experimentally by the reaction of PMe_3 with Ar′HGeGeHAr′ to give the $Ar'(PMe_3)GeGeH_2Ar'$ adduct.[41] Subsequent to its formation, **IM2** reacts with H_2 via passage of the barriers **TS5** and **TS6** to generate the thermodynamically and chemically stable $Ar'H_2GeGeH_2Ar'$ and $Ar'GeH_3$ products. When not enough H_2 is available to react with Ar′HGeGeHAr′, the products could be a mixture of Ar′HGeGeHAr′, $Ar'H_2GeGeH_2Ar'$, and $Ar'GeH_3$. Consistently, the experimental addition of 1 equiv of H_2 to Ar′GeGeAr′ gave Ar′HGeGeHAr′ as the major product (21%), but $Ar'H_2GeGeH_2Ar'$ (10%) and $Ar'GeH_3$ (9%) were also formed in smaller amounts (see eq

dx.doi.org/10.1021/ja300111q | J. Am. Chem. Soc. 2012, 134, 8856−8868

Table 1. Comparisons of the Entropy Contributions ($-T\Delta S$) for the Dissociations and Isomerizations of Ar′HEEHAr′ (E = Ge, Sn) Estimated by the Ideal-Gas-Phase Model and of the Stabilities of the Ge and Sn Species Relative to ArHEEHAr (E = Ge, Sn; Ar = Ar′, Ar*)[a]

	ΔE	ΔH	ΔG	$-T\Delta S^c$	$\Delta G_{corr}{}^d$
Ar′HSnSnHAr′	0.0 (0.0)[b]	0.0	0.0	0.0	0.0
Ar′HSn: + Ar′HSn:	18.4	3.8	−13.8	−17.6	−5.0
Ar′Sn(μ-H)SnHAr′	1.8	−2.4	−3.4	−1.0	−2.9
Ar′SnSnH$_2$Ar′	−0.8 (−2.2)	−5.0	−5.7	−0.7	−5.3
Ar′Sn(μ-H)$_2$SnAr′	−3.8 (4.8)	−8.6	−8.8	−0.2	−8.9
Ar′HGeGeHAr′	0.0	0.0	0.0	0.0	0.0
Ar′HGe: + Ar′HGe:	32.0	20.0	2.3	−17.7	11.2
Ar′Ge(μ-H)GeHAr′	7.7	6.4	6.7	0.3	6.5
Ar′GeGeH$_2$Ar′	2.9	1.4	2.5	1.1	1.9
Ar′Ge(μ-H)$_2$GeAr′	12.0	8.6	8.9	0.3	8.8
Ar*HSnSnHAr*	0.0 (0.0)	0.0	0.0	0.0	0.0
Ar*HSn: + Ar*HSn:	7.2	2.2	−14.7	−16.9	−6.2
Ar*Sn(μ-H)SnHAr*	2.1	0.7	−0.7	−1.4	0.0
Ar*SnSnH$_2$Ar*	−1.0 (−8.9)	−1.1	−3.3	−2.2	−2.2
Ar*Sn(μ-H)$_2$SnAr*	3.2 (5.4)	2.5	2.6	0.1	2.5

[a]The reported values (all in kcal/mol) are based on single-point IEFPCM computations using heptane parameters for the Ge species and toluene parameters for the Sn species, except for the values of ΔE, which are the electronic energies without ZPE corrections. [b]B3PW91 results in the gas phase from ref 24j are given in parentheses. [c]Computed as $\Delta G - \Delta H$. [d]A 0.5 scaling factor was applied to ΔS (but not to ΔG) (see the text).

1).[4] When excess H_2 is present, Ar′HGeGeHAr′ is depleted by further reaction with H_2, affording the thermodynamically and chemically more stable Ar′H_2GeGeH_2Ar′ and Ar′GeH_3 products. Our proposed mechanism and the 0.3 kcal/mol difference between the **TS5** and **TS6** barriers predicts an Ar′H_2GeGeH_2Ar′/Ar′GeH_3 ratio of ca. 56:44, in reasonable agreement with the experimental ratio of 65:35.[4]

Power[18a,b] rationalized the facile H_2 activation by Ar′GeGeAr′ using frontier MO theory. As illustrated in Figure 3A, the occupied out-of-plane π-orbital of Ar′GeGeAr′ interacts with the σ^* antibonding orbital of H_2, and the H_2 σ bonding orbital interacts with the unoccupied in-plane n_+ orbital. The cooperative Lewis acid and base effects split H_2. The same principle applies to H_2 activation by FLPs,[9] carbenes,[15] and even TM complexes.[3] The computed frontier MOs (HOMO and LUMO) of Ar′GeGeAr′ (Figure 3B) support this rationalization. Because the active Ar′GeGeAr′ HOMO has contributions from both Ge atoms, the involvement of both Ge atoms in H_2 activation by Ar′GeGeAr′ (see **TS1**) is reasonable. It should be noted that the HOMO and LUMO of the Jones–Frenking compound LGeGeL, which features a single bond rather than a formal triple Ge–Ge bond,[23] have the reverse order compared with that of Ar′GeGeAr′.

Our computations demonstrate that Ar′HGeGeHAr′ does not react with H_2 because the computed 37.1 kcal/mol activation barrier (**TS3**) is too high. Instead, Ar′HGeGeHAr′ must first isomerize into Ar′GeGeH_2Ar′ (**IM2** in Scheme 2), which is more reactive toward H_2 because of its carbene character. The computed activation barriers from **IM2**, 19.3 (**TS5**) and 19.6 kcal/mol (**TS6**) are 15.3 and 15.0 kcal/mol lower than **TS3**, respectively, based on the same energy reference (Ar′GeGeAr′ + 2H_2). The HOMO and LUMO of Ar′HGeGeHAr′ (Figure 3C) help explain its lower reactivity toward H_2. Unlike the planar carbon sp^2 bonding in ethylene, Ar′HGeGeHAr′ has pyramidal arrangements around the germanium atoms. This germanium pyramidalization diminishes the HOMO π bonding and the LUMO π^* antibonding character significantly, resulting in a much lower barrier for H_2 addition (37.1 kcal/mol) in comparison with the very high barrier (ca. 85.0 kcal/mol[11a]) for H_2 addition to ethylene. The high barrier of the latter is due to the symmetry-forbidden interactions of the ethylene π HOMO and π^* LUMO with the respective σ^* and σ orbitals of H_2. Although diminished, the same unfavorable orbital interactions exist and inhibit the addition of H_2 to Ar′HGeGeHAr′, resulting in its low reactivity.

The Ge(II) hydride Ar′GeGeH_2Ar′ (**IM2**) has carbene character (as shown by the HOMO and LUMO in Figure 3D); its high reactivity toward H_2 via **TS5** is, in principle, like that of the (alkyl)(amino) carbenes. Bertrand[15] attributed H_2 activation by the latter to the synergetic interactions between the occupied in-plane carbene lone-pair orbital and the H_2 σ^*

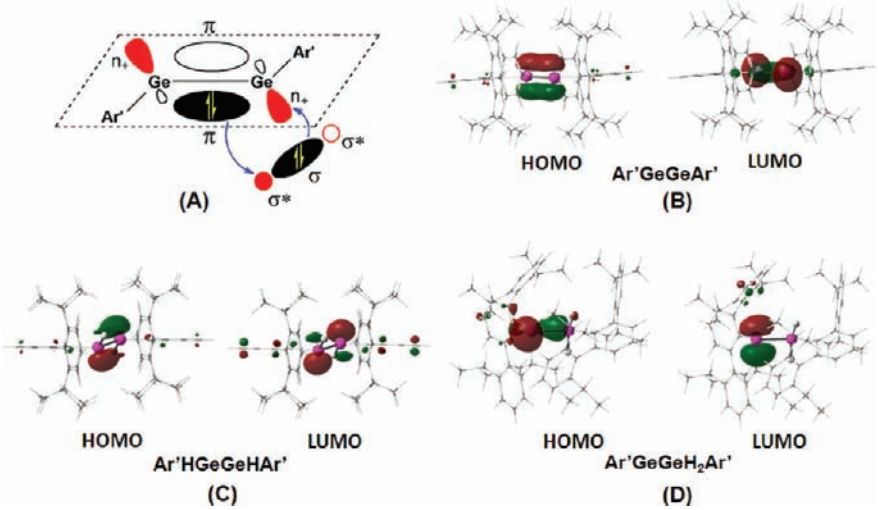

Figure 3. (A) Symmetry-allowed orbital interactions between H_2 and Ar′GeGeAr′ proposed by Power.[18a,b] (B) HOMO and LUMO of Ar′GeGeAr′. (C) HOMO and LUMO of Ar′HGeGeHAr′. (D) HOMO and LUMO of Ar′GeGeH_2Ar′.

dx.doi.org/10.1021/ja300111q | J. Am. Chem. Soc. 2012, 134, 8856–8868

antibonding orbtial and between the out-of-plane unoccupied carbene carbon p AO and the H_2 σ bonding orbital. The same principle can be applied to explain the high reactivity of Ar′GeGeH$_2$Ar′ toward H_2 via **TS5**. However, the Ar′-Ge^{a}Ge^{b}H$_2$Ar′ HOMO is not a pure localized Ge^a lone pair but involves the σ bonding electrons of the Ge^a−Ge^b bond. The combination of the lone-pair-like electrons on Ge^a (red) and the Ge−Ge σ bonding electrons (green) symmetrically allow the H_2 σ* antibonding orbital to interact with the HOMO. Similar to the activation mode via **TS5**, the LUMO of Ar′GeGeH$_2$Ar′ also can interact with the H_2 σ bonding orbital. The synergistic orbital interactions result in activation via **TS6**. Because this activation mode involves the σ bonding electrons of the Ge^a−Ge^b bond, one of the H atoms of H_2 should be closer to Ge^b in **TS6** than in **TS5**. Consistently, the H^b−Ge^b distance of 2.664 Å in **TS5** is longer than the distance of 2.027 Å in **TS6** (see Figure 2). Furthermore, the donation of the σ bonding electrons of the Ge^a−Ge^b bond to the H_2 σ* antibonding orbital weakens the Ge−Ge bond (the Ge^a−Ge^b distance is 2.625 Å in **TS6**), which eventually breaks to give Ar′HGe: + Ar′GeH$_3$.

3.2. Reaction Mechanism of Ar′SnSnAr′/Ar*SnSnAr* with H_2 (eqs 2 and 3). In striking contrast to the digermyne Ar′GeGeAr′, which can react with 1−3 equiv of H_2 to give mixtures of the products Ar′HGeGeHAr′, Ar′H$_2$GeGeH$_2$Ar′ and Ar′GeH$_3$ (eq 1),[4] the distannyne Ar′SnSnAr′ reacts only with 1 equiv of H_2 to give doubly H-bridged Ar′Sn(μ-H)$_2$SnAr′ as the sole product (eq 2).[21] Ar′HSnSnHAr′, Ar′H$_2$SnSnH$_2$Ar′, and Ar′SnH$_3$ (the Sn counterparts of Ar′HGeGeHAr′, Ar′H$_2$GeGeH$_2$Ar′, and Ar′GeH$_3$ in eq 1) are not formed, even with excess H_2.[21] Power and co-workers[21] proposed a reaction sequence for the reaction (Scheme 3). The activation of H_2 at a single Sn site of Ar′SnSnAr′ leads to the asymmetric Sn(II) hydride Ar′SnSnH$_2$Ar′, which then rearranges to give doubly H-bridged Ar′Sn(μ-H)$_2$SnAr′.

Scheme 3. Reaction Sequence for the Reaction of Ar′SnSnAr′ with H_2 (eq 2) Proposed by Power and Co-workers[21]

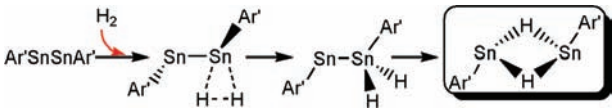

Scheme 4 presents our computed energetic results for the reaction shown in eq 2. The optimized structures of key stationary points are displayed in Figure 4 (see section SI10 for the rest). Like the activation of H_2 by Ar′GeGeAr′ (see **TS1**), the Sn−Sn bond of Ar′SnSnAr′, rather than a single Sn atom, is the active site (**TS13**). This is reflected by the optimized geometry of **TS13** (Figure 4) and was confirmed by examining the harmonic vibrational mode corresponding to the imaginary frequency (see section SI11). Attempts to locate a transition state for H_2 activation by a single Sn site of Ar′SnSnAr′ using different initial geometries converged repeatedly to the separated Ar′SnSnAr′ + H_2 species or gave the same transition state structure (**TS13**). The H_2 activation barrier via **TS13** (14.4 kcal/mol) is smaller than that for H_2 activation by Ar′GeGeAr′ (**TS1**, 18.4 kcal/mol).

As in the case of Ar′GeGeAr′, H_2 activation by Ar′SnSnAr′ gives the singly H-bridged intermediate Ar′Sn(μ-H)SnHAr′ (**IM5**) and is exergonic by 8.9 kcal/mol, compared with 10.5 kcal/mol for the corresponding intermediate **IM1** in the Ar′GeGeAr′ + H_2 reaction (Scheme 2). The production of singly H-bridged Ar′Sn(μ-H)SnHAr′ agrees with the existence of the singly bridged HSn(μ-H)SnH$_2$ local minimum on the Sn$_2$H$_4$ potential energy surface predicted by Trinquier.[43] However, they did not identify the HGe(μ-H)GeH$_2$ counterpart.[43] We optimized the HGe(μ-H)GeH$_2$ structure and found that it also is a local minimum at the TPSSTPSS, MP2, and CCSD(T)/BSI levels (section SI12), supporting the idea that H_2 activation by Ar′GeGeAr′ involves singly bridged Ar′Ge(μ-H)GeHAr′.

Three pathways [**A** (red), **B** (black), and **C** (blue) in Scheme 4] can lead from **IM5** to the 5.4 kcal/mol more stable experimental product Ar′Sn(μ-H)$_2$SnAr′ (shown in the box in Scheme 4). Pathway **A** from **IM5** passes through a low barrier (**TS14**, 10.4 kcal/mol) involving H^b movement to the bridging position and generates the Ar′Sn(μ-H)$_2$SnAr′ product directly. However, pathway **B** has an even lower barrier from **IM5** (**TS15**, 4.8 kcal/mol) and gives **IM6** (Ar′HSnSnHAr′), which then dissociates into two Ar′HSn: species (**IM7**). As detailed in section SI13, the potential (electronic) energy surface for **IM6** dissociation [Ar′HSnSnHAr′ → **IM7** + **IM7** (Ar′HSn:)] increases monotonically. In terms of enthalpy, **IM7** + **IM7** is 3.7 kcal/mol higher than **IM6**. However, because the dissociation is entropically favorable, **IM7** + **IM7** is 13.8 kcal/mol lower than **IM6** in terms of free energy, indicating that the dissociation of **IM6** is facile. The two resulting **IM7** species then reassemble, giving the product, Ar′Sn(μ-H)$_2$SnAr′. Evidently, the carbene analogue **IM7** cannot activate H_2, since the barrier (**TS16**, 41.3 kcal/mol) is too high. Pathway **C** involves the transformation of **IM5** into **IM8** (Ar′SnSnH$_2$Ar′) via a low barrier (**TS17**, 3.2 kcal/mol). However, **IM8** must overcome a 26.4 kcal/mol barrier (**TS18**) to reach the product. The energetics of the three alternatives (Scheme 4) favor pathway **B**. This mechanism also is supported by a recent experimental and computational study of the reaction of Ar′$_2$Sn: and H_2 in which Ar′HSn: and Ar′H form first and then two Ar′HSn: species associate to give the Ar′Sn(μ-H)$_2$SnAr′ product.[25] Another experiment reported that the monomer Ar$^\#$ClSn: [Ar$^\#$ = 2,6-(2,4,6-*i*Pr$_3$C$_6$H$_2$)$_2$C$_6$H$_3$] could be associated with the doubly Cl-bridged Ar$^\#$Sn(μ-Cl)$_2$Ar$^\#$.[42]

At first glance, the predicted pathway **B** (Scheme 4 and Table 1) seems energetically inconsistent with the crystallization of Ar′Sn(μ-H)$_2$SnAr′ because the free energy of Ar′HSn: + Ar′HSn: is 5.0 kcal/mol lower than Ar′Sn(μ-H)$_2$SnAr′ (although the former is 12.4 kcal/mol in enthalpy higher than the latter). We analyzed the following factors that could be responsible for the inconsistency. First, the computations did not take the crystal packing effect into account. Power, Nagase, Herber, and co-workers reasoned that the packing forces could be very important in dictating which structure among several energetically close organotin(II) hydride isomers can be crystallized.[24j] Second, it is well-rrecognized that the ideal-gas-phase computational methods overestimate entropic contributions in solution,[44] particularly for dissociation processes. An experimental study has shown that this inherent overestimation could be 50−60% of the total entropic contribution.[44e] Accurate entropy estimations in solution are still a challenge for theoretical chemistry.[45] The Ar′HSnSnHAr′ → Ar′HSn: + Ar′HSn: dissociation is entropically favorable because a single component is transformed into two. However, the freedom of movement of each individual species is restricted by adjacent solvent molecules. This effect, which diminishes the entropy, is not taken into account in computations using the gas-phase

dx.doi.org/10.1021/ja300111q | J. Am. Chem. Soc. 2012, 134, 8856−8868

Scheme 4. Free Energy Profile for the Reaction of Ar′SnSnAr′ with H_2 (eq 2)[a]

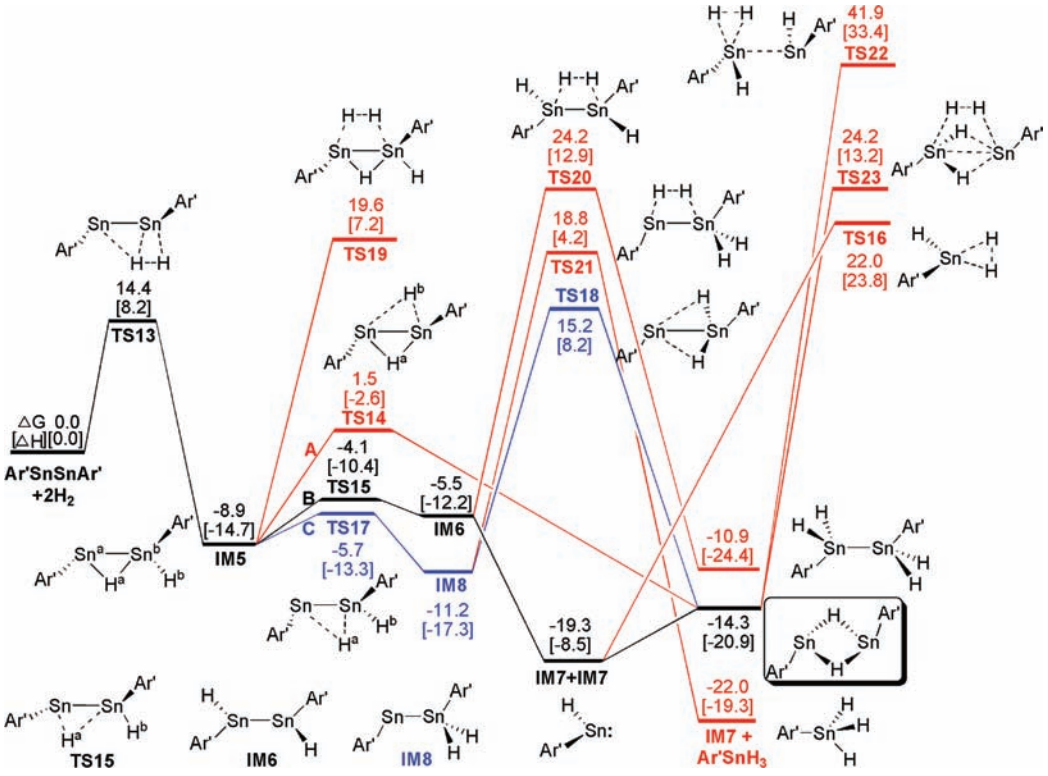

[a]Values shown are relative free energies, with enthalpies given in square brackets (all in kcal/mol). The pathway leading to the experimental product (enclosed in the box) is shown in black. The pathway corresponding to the sequence proposed by Power and co-workers[21] is shown in blue. Other unfavorable pathways are shown in red.

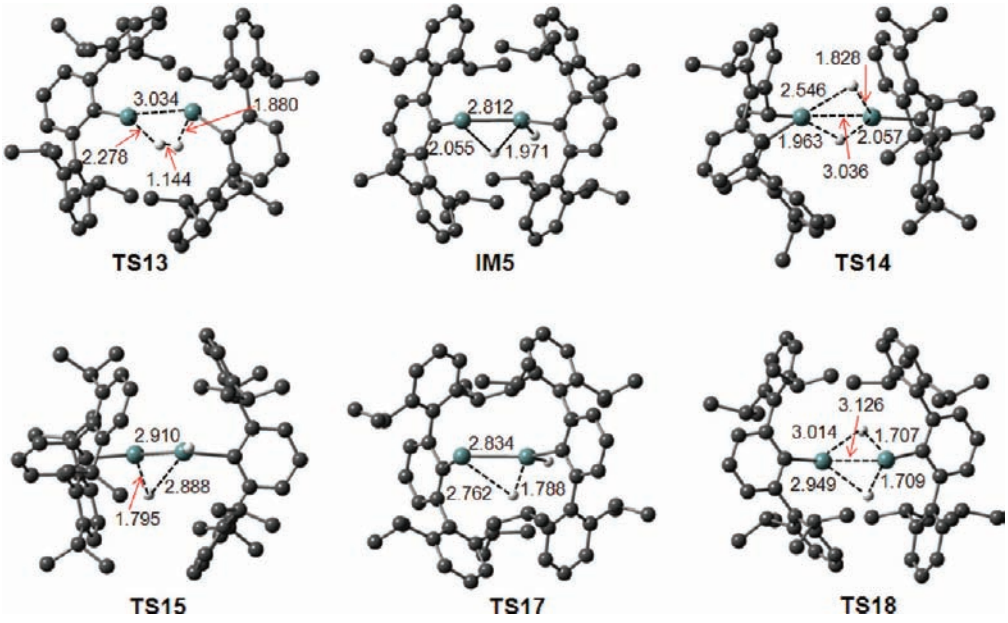

Figure 4. Optimized structures of some of the stationary points in Scheme 4, along with the key bond distances in Å. Other optimized structures are given in section SI10. Trivial H atoms have been omitted for clarity. Color code: C, black; H, white; Sn, dark-green.

model. The flaws in such uncorrected computations are emphasized by the $-T\Delta S$ values in Table 1 (which correspond to $\Delta G - \Delta H$); these are much larger for the Ar′HEEHAr′ (E = Sn, Ge) dissociations (ca. −17.0 kcal/mol) than for the various isomerization processes (−2.2 to 1.1 kcal/mol). However, if the experimentally derived scaling factor (0.5) is applied,[44e] for example, to the entropic contribution (−17.6 kcal/mol), ΔG_{corr} in Table 1 for Ar′HSn: + Ar′HSn: is 3.9 kcal/mol higher than that for Ar′Sn(μ-H)$_2$SnAr′. Thus, Ar′Sn(μ-H)$_2$SnAr′ is more stable than Ar′HSn: + Ar′HSn: in solution. On the basis of the corrected free energy values (ΔG_{corr}), Ar′HGeGeHAr′ is 11.2 kcal/mol more stable than Ar′HGe: + Ar′HGe: (see the

dx.doi.org/10.1021/ja300111q | J. Am. Chem. Soc. 2012, 134, 8856−8868

discussion of the feasibility of the Ar′HGe: + Ar′HGe: → Ar′HGeGeHAr′ dimerization in section 3.1), implying that the direct dissociation of Ar′HGeGeHAr′ to give two Ar′HGe: species is an unfavorable process. The analysis of the free energy profiles in Schemes 2 and 4 holds true when the overestimation of the entropic contributions is taken into account. The scaled free energy profiles corresponding to Schemes 2 and 4 are given in section SI14. Third, because crystals are in the solid state, where the translational and rotational motions of the molecules are greatly restricted, the entropic contribution in favor of dissociation should be even smaller than that in solution. If the entropy contribution is excluded, Ar′Sn(μ-H)$_2$SnAr′ is 12.4 kcal/mol lower in enthalpy than **IM7** + **IM7** (see Table 1 and below).

The **IM5** → **TS17** → **IM8** step along pathway **C** (Scheme 4) is more favorable, both kinetically and thermodynamically, than the **IM5** → **TS15** → **IM6** step along pathway **B**. Consequently, **IM8** might be generated in situ. We propose that **IM8** reverts to **IM5** and then follows the overall energetically more favorable pathway **B** (**TS15** → **IM6** → **IM7** + **IM7**, colored in black) to give the Ar′Sn(μ-H)$_2$SnAr′ product because the following two possible pathways from **IM8** to Ar′Sn(μ-H)$_2$SnAr′ are less favorable. The direct rearrangement of **IM8** to give Ar′Sn(μ-H)$_2$SnAr′ would require a crossing of barrier **TS18**, which is 19.3 kcal/mol higher than **TS15**. Alternatively, **IM8** may dissociate first into two radicals (Ar′Sn· + Ar′H$_2$Sn·), which could then reassemble into Ar′Sn(μ-H)$_2$SnAr′. Because the dissociation products are 4.4 kcal/mol higher than **TS15** (or 12.9 kcal/mol higher if the overestimation of the entropy contribution is corrected by applying a scaling factor of 0.5 to $-T\Delta S$[44e]), this pathway is also less favorable.

In addition to the pathways leading to the experimental product Ar′Sn(μ-H)$_2$SnAr′, we also considered other possible reactions (also shown in red in Scheme 4), including the reactions of **IM5** with H$_2$ via **TS19**, **IM6** with H$_2$ via **TS20**, **IM8** with H$_2$ via **TS21**, **IM7** with H$_2$ via **TS16**, and Ar′Sn(μ-H)$_2$SnAr′ with H$_2$ via **TS22** or **TS23**. The computed barriers exclude these possibilities, further demonstrating the exclusive production of Ar′Sn(μ-H)$_2$SnAr′ by the reaction shown in eq 2.

The mechanism for the Ar′SnSnAr′ + H$_2$ → Ar′Sn(μ-H)$_2$SnAr′ addition (eq 2) helps us understand why the reaction of Ar*SnSnAr* with H$_2$ (eq 3) gives the Sn(II) hydride Ar*SnSnH$_2$Ar* as the final product.[21] The large size of Ar*SnSnH$_2$Ar* (210 atoms) prevented us from characterizing the pathways in detail as we did for those for eq 2. Inspired by the work of Power, Nagase, Herber, and co-workers[24j] showing that the size of the aryl group could alter the relative stabilities of the isomers ArHSnSnHAr, ArSnSnH$_2$Ar, and ArSn(μ-H)$_2$SnAr (Ar = Ar′, Ar*), we compared the relative stabilities of the five minima obtained when Ar′ is replaced by Ar* (i.e., Ar*HSnSnHAr*, Ar*HSn: + Ar*HSn:, Ar*Sn(μ-H)SnHAr*, Ar*SnSnH$_2$Ar*, and Ar*Sn(μ-H)$_2$SnAr*) at the current level.

We first examined the relative stabilities of the two key isomers, namely, doubly H-bridged Ar*Sn(μ-H)$_2$SnAr* [the counterpart of the experimentally observed Ar′Sn(μ-H)$_2$SnAr′] and the experimental product Ar*SnSnH$_2$Ar*. The optimized structures of the two minima are displayed in Figure 5. The geometry of Ar*SnSnH$_2$Ar* agrees well with its X-ray crystal structure.[21] As expected, the more bulky Ar* substituent elongates the Sn−Sn bonds in Ar*SnSnH$_2$Ar* and Ar*Sn(μ-H)$_2$SnAr* to 2.982 Å and 3.265 Å, respectively, compared with the respective values in Ar′SnSnH$_2$Ar′ (**IM8**) and Ar′Sn(μ-H)$_2$SnAr′ (2.944 Å and 3.189 Å) (see section SI10).

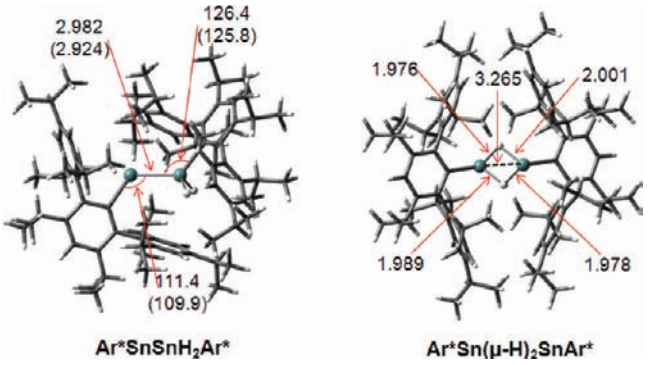

Figure 5. Optimized structures of Ar*SnSnH$_2$Ar* and Ar*Sn(μ-H)$_2$SnAr*, along with the key bond distances in Å. X-ray values[21] (in parentheses) also are given for Ar*SnSnH$_2$Ar*. Trivial H atoms and all of the C atoms are shown as sticks for clarity.

The Ar′ and Ar* substituents result in relative energy differences (Table 1). While Ar′Sn(μ-H)$_2$SnAr′ is 3.1 kcal/mol *more* stable than Ar′SnSnH$_2$Ar′, Ar*Sn(μ-H)$_2$SnAr* is 5.9 kcal/mol *less* stable than Ar*SnSnH$_2$Ar*. The reversal in the relative stabilities of the two isomers can be attributed to the increased steric effect in Ar*Sn(μ-H)$_2$SnAr* relative to Ar*SnSnH$_2$Ar*, which is supported by the greater elongation of the Sn−Sn distance in Ar*Sn(μ-H)$_2$SnAr* versus Ar′Sn(μ-H)$_2$SnAr′ (0.076 Å) relative to that in Ar*SnSnH$_2$Ar* versus Ar′SnSnH$_2$Ar′ (0.038 Å). The pathway leading to Ar′Sn(μ-H)$_2$SnAr′ in the reaction of Ar′SnSnAr′ and H$_2$ (Scheme 4) is 1.6 kcal/mol less favorable kinetically (**TS15** vs **TS17**) but 3.1 kcal/mol more favorable thermodynamically [**IM8** vs Ar′Sn(μ-H)$_2$SnAr′] than the pathway leading to Ar′SnSnH$_2$Ar′ (**IM8**). Because the replacement of Ar′ with Ar* stabilizes Ar*SnSnH$_2$Ar* relative to Ar*Sn(μ-H)$_2$SnAr* for the reaction of Ar*SnSnAr* and H$_2$ (eq 3), we can infer that this replacement also stabilizes the transition state corresponding to **TS17** (Scheme 4). Therefore, the pathway leading to Ar*SnSnH$_2$Ar* in the Ar*SnSnAr* + H$_2$ reaction could be both kinetically and thermodynamically more favorable than that leading to Ar*Sn(μ-H)$_2$SnAr*. As shown in Scheme 4, the Ar′SnSnH$_2$Ar′ ⇄ Ar′Sn(μ-H)$_2$SnAr′ isomerization via **TS15** is facile [the barrier is 7.1 (forward) and 10.2 kcal/mol (backward); the equilibrium favors Ar′Sn(μ-H)$_2$SnAr′]. As the replacement of Ar′ with Ar* is not expected to influence the ease of the Ar*SnSnH$_2$Ar* ⇄ Ar*Sn(μ-H)$_2$SnAr* isomerization, this equilibrium should favor the more stable Ar*SnSnH$_2$Ar* (the experimental product). The latter should thus result even if Ar*Sn(μ-H)$_2$SnAr* is formed initially.

The relative energies of the two sets of five isomers ArHSnSnHAr, HArSn: + HArSn:, ArSn(μ-H)SnHAr, ArSnSnH$_2$Ar, and ArSn(μ-H)$_2$SnAr (Ar = Ar′, Ar*) are compared in Table 1, and their optimized structures are shown in Figure 4 and section SI10 (Ar = Ar′) and Figure 5 and section SI15 (Ar = Ar*). The B3PW91 energies ΔE [relative electronic energies in the gas phase without zero-point energy (ZPE) corrections] of Power, Nagase, Herber, and co-workers[24j] are also included for comparison. According to the B3PW91 ΔE values for Ar = Ar′, the Sn(II) hydride (Ar′SnSnH$_2$Ar′) is most stable, rather than the experimentally found Ar′Sn(μ-H)$_2$SnAr′.[24j] This disagreement was attributed to possible crystal packing forces.[24j] However, our TPSSTPSS computations of ΔE, ΔH, and ΔG_{corr} values (Table 1) predict that Ar′Sn(μ-H)$_2$SnAr′ should be the most stable. For Ar = Ar*, both the B3PW91[24j]

dx.doi.org/10.1021/ja300111q | J. Am. Chem. Soc. 2012, 134, 8856−8868

Table 2. Comparisons of the Reactivities of Various Ge and Sn Species toward H_2

Ge species	ΔG [ΔH]	TS	Sn species	ΔG [ΔH]	TS
Ar′GeGeAr′	18.4 [8.2]	**TS1**	Ar′SnSnAr′	14.4 [8.2]	**TS13**
Ar′HGeGeHAr′	37.1 [28.2]	**TS3**	Ar′HSnSnHAr′	29.7 [25.1]	**TS20**
Ar′GeGeH$_2$Ar′	19.3 [11.7]	**TS5**	Ar′SnSnH$_2$Ar′	–[a]	–[a]
Ar′GeGeH$_2$Ar′	19.6 [11.8]	**TS6**	Ar′SnSnH$_2$Ar′	30.0 [21.5]	**TS21**
Ar′HGe:	24.7 [15.8]	**TS7**	Ar′HSn:	41.2 [32.4]	**TS16**
Ar′Ge(μ-H)$_2$GeAr′	37.2 [36.2]	**TS9**	Ar′Sn(μ-H)$_2$SnAr′	56.2 [54.3]	**TS22**
Ar′Ge(μ-H)$_2$GeAr′	38.9 [31.0]	**TS10**	Ar′Sn(μ-H)$_2$SnAr′	38.5 [34.1]	**TS23**

[a]Transition state computation trials using a single Sn site in Ar′SnSnH$_2$Ar′ repeatedly converged to **TS21**, which uses a joint Sn−Sn site.

and TPSSTPSS computations agree that Ar*SnSnH$_2$Ar* is more stable than Ar*Sn(μ-H)SnHAr*, Ar*HSnSnHAr*, and Ar*Sn(μ-H)$_2$SnAr*. However, the bimolecular minimum (Ar*HSn: + Ar*HSn:) is 11.4 kcal/mol (in ΔG) and 4.0 kcal/mol (in ΔG_{corr}) lower than Ar*SnSnH$_2$Ar*. Similar to the Ar′ case, we attribute the inconsistency between the relative free energies and the Ar*SnSnH$_2$Ar* X-ray structure to the fact that the free energy contribution (mainly due to translational and rotational motions) in favor of the bimolecular minimum could be greatly limited in the solid state. Indeed, if the entropy contributions are excluded, Ar*SnSnH$_2$Ar* is enthalpically most stable among the five minima (see Table 1). According to the ΔG_{corr} value of −4.0 kcal/mol for Ar*SnSnH$_2$Ar* → Ar*HSn: + Ar*HSn: approximately estimated in the solvent, we speculate that Ar*HSn: species could exist in solution but that the crystallization condition (solid state) leads to the enthalpically more stable Ar*SnSnH$_2$Ar*. As this speculation needs further experimental verification, we examined whether our analyses could explain another experiment of Power and co-workers,[42] who reported that although doubly Cl-bridged Ar#Sn(μ-Cl)$_2$SnAr# dissociates into two Ar#ClSn: monomers in solution (C_6D_6), they obtained crystal structures of both Ar#Sn(μ-Cl)$_2$SnAr# and Ar#ClSn:. At the same level, we computed the thermodynamics of the dissociation process Ar#Sn(μ-Cl)$_2$SnAr# → Ar#ClSn: + Ar#ClSn:. The optimized structures involved are given in section SI16. The Ar#Sn(μ-Cl)$_2$SnAr# structure was predicted to be 0.9 kcal/mol (in ΔH) more stable than Ar#ClSn: + Ar#ClSn:. The small enthalpy difference is in agreement with the observation that both Ar#Sn(μ-Cl)$_2$SnAr# and Ar#ClSn: could be obtained in X-ray experiments. In terms of the free energies in solution, Ar#Sn(μ-Cl)$_2$SnAr# is 13.4 kcal/mol (ΔG) and 6.3 (ΔG_{corr}) less stable than Ar#ClSn: + Ar#ClSn:, indicating that the monomers should be preferred in solution, in agreement with the experimental results.[42] Because the values of ΔG (−13.4 kcal/mol) and ΔG_{corr} (−6.3 kcal/mol) for Ar#Sn(μ-Cl)$_2$SnAr# → Ar#ClSn: + Ar#ClSn: are comparable to those for Ar*SnSnH$_2$Ar* → Ar*HSn: + Ar*HSn: (−11.4 and −4.0 kcal/mol, respectively), Ar*SnSnH$_2$Ar* could also exist as Ar*HSn: monomers in solution but under crystallization conditions exist as the enthalpically more stable Ar*SnSnH$_2$Ar* (see Table 1).

3.3. Further Discussion of the Differences between the Reactions in eqs 1 and 2. The mechanisms of the reactions in eqs 1 and 2 rationalize the formation of the corresponding experimental products. In general, the differences between these reactions arise because the Sn lone pair is more stable than the Ge lone pair (the inert pair effect)[46] and Sn is more metallic than Ge. Because of these differences, Ar′Sn(μ-H)$_2$SnAr′ in eq 2 and Ar*SnSnH$_2$Ar* in eq 3 are the preferred products (thermodynamically more stable) for the additions of H_2 to Ar′SnSnAr′ and Ar*SnSnAr*, but neither can react further with H_2. In contrast, Ar′Ge(μ-H)$_2$GeAr′ is the least stable among its isomers (Table 1), and addition of H_2 to Ar′GeGeAr′ prefers to give the more stable species Ar′HGeGeHAr′ or Ar′GeGeH$_2$Ar′. The latter has an electronic structure (more active lone pair) suitable to react further with H_2, and the 2.5 kcal/mol more stable Ar′HGeGeHAr′ can also further react with H_2 indirectly via a facile isomerization to Ar′GeGeH$_2$Ar′.

On the basis of the computed kinetics and thermodynamics of these two reactions (Schemes 2 and 4), we can further analyze in more detail why they form completely different products. (I) Ar′HGeGeHAr′ could be observed with 1 equiv of H_2 in eq 1, but its counterpart Ar′HSnSnHAr′ could not in eq 2. This occurs because Ar′HSnSnHAr′ (**IM6**) is less stable than the other possible isomers [i.e., **IM5**, **IM8**, **IM7** + **IM7**, and Ar′Sn(μ-H)$_2$SnAr′] and can be transformed to the more stable Ar′Sn(μ-H)$_2$SnAr′ facilely. In contrast, Ar′HGeGeHAr′ is more stable than other possible isomers (i.e., **IM1**, **IM2**, **IM4**, and **IM3** + **IM3**) (Table 1). (II) Ar′H$_2$GeGeH$_2$Ar′ (eq 1) but not Ar′H$_2$SnSnH$_2$Ar′ (eq 2) could be observed. This occurs because the pathways leading to Ar′H$_2$SnSnH$_2$Ar′ (including **IM5** + H_2 via **TS19** and **IM6** + H_2 via **TS20**) are unfavorable or less favorable than the pathway leading to Ar′Sn(μ-H)$_2$SnAr′ (see Scheme 4), while the pathway leading to Ar′H$_2$GeGeH$_2$Ar′ (shown in black in Scheme 2) is the most kinetically and thermodynamically favorable. (III) Ar′GeH$_3$ was observed in eq 1, but Ar′SnH$_3$ was not in eq 2. This occurs because the pathways **IM6** → **TS21** → **IM7** + Ar′SnH$_3$ and Ar′Sn(μ-H)$_2$SnAr′ → **TS22**/**TS23** → **IM7** + Ar′SnH$_3$/Ar′SnH$_3$ + Ar′SnH$_3$ (Scheme 4) are less favorable than that leading to Ar′Sn(μ-H)$_2$SnAr′. In addition, because **TS21**/**TS22**/**TS23** are 22.9/46.0/28.3 kcal/mol higher than **TS15**, the products **IM7** + Ar′SnH$_3$, which are 7.7 kcal/mol more stable than Ar′Sn(μ-H)$_2$SnAr′, cannot be produced. In contrast, **IM2** can react with H_2 to give Ar′GeH$_3$ + Ar′HGe: only by passing over a 19.6 kcal/mol barrier (**TS6**). (IV) Ar′Sn(μ-H)$_2$SnAr′ is the only product in eq 2, but the Ge counterpart Ar′Ge(μ-H)$_2$GeAr′ (**IM4**) does not appear in eq 1. This occurs because the formation of **IM4** is kinetically and thermodynamically less favorable than the pathways leading to Ar′HGeGeHAr′ and **IM2** (Scheme 2). Even if it could be formed, it would isomerize to give the more stable **IM2** and Ar′HGeGeHAr′. In contrast, the pathway leading to Ar′Sn(μ-H)$_2$SnAr′ is the most favorable, and the product is more stable than other possible isomers.

Table 2 aids the experimental development of group 14 compounds for hydrogen activation/hydrogenation by comparing the reactivities (via the activation barriers toward H_2) of the various Ge and Sn species. (I) Ar′GeGeAr′ is slightly less reactive than Ar′SnSnAr′, but both can activate H_2 easily. Because the enthalpy barriers of the two molecules are the same

dx.doi.org/10.1021/ja300111q | J. Am. Chem. Soc. 2012, 134, 8856−8868

(8.0 kcal/mol), the entropic contribution rather than the electronic effect is the major factor responsible for the large difference in the free energy barriers (18.4 vs 14.4 kcal/mol). The comparable enthalpy barriers do not contradict to the inert pair effect[46] because the H_2 activations by the heavier alkyne analogues involve the π bonding orbitals (the HOMO in Figure 3B) rather than the lone pair. Previously, simplified CH_3EECH_3 (E = Si−Pb) models were used to investigate the reactivities of the heavier alkyne analogues,[24k] and it was found that Ar′GeGeAr′ has more significant diradical character than its Sn counterpart.[24k] However, as noted in Computational Details, the wavefunctions of Ar′GeGeAr′ and Ar′SnSnAr′ were confirmed to be stable, which implies the experimental systems have no significant diradical character. Takagi and Nagase[24i] found that the simplified models could not represent the real systems well; the $CH_3SnSnCH_3$ model does not even have a local minimum close to the X-ray structure of Ar′SnSnAr′. (II) Both Ar′HGeGeHAr′ and Ar′HSnSnHAr′ have high activation barriers (37.1 and 29.7 kcal/mol, respectively) and cannot activate H_2 under ambient conditions. Similar to the case of Ar′GeGeAr′ versus Ar′SnSnAr′, the enthalpy barriers of the two molecules are comparable (28.2 vs 25.1 kcal/mol). (III) Ar′GeGeH$_2$Ar′ can activate H_2 via a single Ge site or a joint Ge−Ge site with surmountable barriers (**TS5** and **TS6**, ca. 19.5 kcal/mol). The reaction of Ar′SnSnH$_2$Ar′ with H_2 can take place only on a Sn−Sn site, and the barrier (**TS21**, 30.0 kcal/mol) is much higher than that for Ar′GeGeH$_2$Ar′ (**TS6**, 19.6 kcal/mol). The higher reactivity of Ar′GeGeH$_2$Ar′ in comparison with Ar′SnSnH$_2$Ar′ results because the H_2 activations by Ar′E^{a}E^{b}H$_2$Ar′ involve the use of the nonbonding lone pair on E^a, but the Sn lone pair is more stable than the Ge lone pair because of the inert pair effect.[46] As mentioned above, the higher reactivity toward H_2 for Ar′GeGeH$_2$Ar′ in comparison with Ar′SnSnH$_2$Ar′ is the origin for the differences between the reactions in eqs 1 and 2. Because of the low reactivity of Ar′SnSnH$_2$Ar′, its reaction with H_2 to give **IM7** + Ar′SnH$_3$ via **TS21** does not take place, even though **IM7** + Ar′SnH$_3$ is 7.7 kcal/mol thermodynamically more favorable than the observed Ar′Sn(μ-H)$_2$SnAr′, and the H_2 addition to the single Sn site leading to Ar′H$_2$SnSnH$_2$Ar′ also cannot occur. From the experimental fact that Ar′GeGeAr′ can react with up to 3 equiv of H_2 while Ar′SnSnAr′ can react only with 1 equiv of H_2, it seems that Ar′GeGeAr′ is more reactive than Ar′SnSnAr′. On the basis of the present study, the seemingly higher reactivity of Ar′GeGeAr′ in comparison with Ar′SnSnAr′ is essentially due to the higher reactivity of Ar′GeGeH$_2$Ar′ in comparison with Ar′SnSnH$_2$Ar′. In fact, the free energy barrier for H_2 activation by Ar′GeGeAr′ is higher than that by Ar′SnSnAr′ (18.4 vs 14.4 kcal/mol). (IV) The Ar′HGe: carbene congener is reactive toward H_2 (24.7 kcal/mol barrier), but the 41.2 kcal/mol activation barrier for Ar′HSn: is too high for H_2 activation. As in the case of Ar′GeGeH$_2$Ar′ versus Ar′SnSnH$_2$Ar′, the large difference in the barriers can be ascribed to the inert pair effect.[46] The experimental behavior is also consistent:[25] while Ar′$_2$Ge: reacts with 2 equiv of H_2 via the intermediate Ar′HGe: to give Ar′GeH$_3$, the Sn analogue Ar′$_2$Sn: can react only with 1 equiv of H_2 via the Ar′HSn: intermediate to give doubly H-bridged Ar′Sn(μ-H)$_2$SnAr′. (V) The reaction barriers of doubly H-bridged Ar′Ge(μ-H)$_2$GeAr′ and Ar′Sn(μ-H)$_2$SnAr′ are large (>35 kcal/mol), and both compounds are inert toward H_2.

CONCLUSIONS

Tests of various combinations of DFT functionals and basis sets led to the choice of the TPSSTPSS/BSII//TPSSTPSS/BSI computational level to investigate details of the reaction mechanisms of H_2 with Ar′GeGeAr′, Ar′SnSnAr′, and Ar*SnSnAr* involving the very bulky substituents needed for experimental success. Our detailed mechanistic study provides insights into the different reactivities of the digermyne and distannynes toward H_2. The reaction of Ar′GeGeAr′ with H_2 takes place in steps: First, H_2 adds to Ar′GeGeAr′ to give singly H-bridged Ar′Ge(μ-H)GeHAr′. The latter isomerizes to the more reactive Ge(II) hydride Ar′GeGeH$_2$Ar′, which then reacts with H_2 either at a single Ge site to give Ar′GeH$_3$ + Ar′HGe: or at a joint Ge−Ge bond to give Ar′H$_2$GeGeH$_2$Ar′. The intermediate Ar′Ge(μ-H)GeHAr′ also can isomerize to the kinetically stable Ar′HGeGeHAr′. Our mechanism predicts a final Ar′H$_2$GeGeH$_2$Ar′/Ar′GeH$_3$ product ratio of 56:44, in reasonable agreement with the 65:35 experimental ratio. The mechanisms of H_2 activation by Ar′SnSnAr′ and Ar′GeGeAr′ are similar. The initially obtained singly H-bridged Ar′Sn(μ-H)SnHAr′ intermediate first isomerizes into Ar′HSnSnHAr′. Subsequent facile dissociation of Ar′HSnSnHAr′ to give Ar′HSn: + Ar′HSn: fragments is followed by their reassembly into the experimental product, Ar′Sn(μ-H)$_2$SnAr′. The reaction of Ar*SnSnAr* with H_2 gives Ar*SnSnH$_2$Ar*, mainly because of its greater stability in comparison with Ar*Sn(μ-H)$_2$SnAr*. The computed reaction energies successfully elucidate the Ar′GeGeAr′, Ar′SnSnAr′, and Ar*SnSnAr* reactivity differences toward H_2.

Our mechanistic study affords further insights. There are similarities and differences in the behavior of analogous Ge and Sn species. (I) The Ar′EEAr′ (E = Ge, Sn) active sites involve both E atoms, and their initial products with H_2 are the singly H-bridged Ar′E(μ-H)EHAr′ species rather than Ar′HEEHAr′ or Ar′EEH$_2$Ar′. (II) Neither the Ar′HEEHAr′ alkene congeners nor the doubly H-bridged Ar′E(μ-H)$_2$EAr′ (E = Ge, Sn) isomers are effective in activating H_2 directly. (III) While Ar′HGeGeHAr′ can isomerize to give Ar′GeGeH$_2$Ar′, which then can react further with H_2 on a single Ge site or at a Ge−Ge bond, the rearranged Ar′SnSnH$_2$Ar′ is not reactive toward H_2. The higher reactivities of Ar′GeGeH$_2$Ar′ and Ar′HGe: relative to their Sn counterparts can be attributed to the inert pair effect. The experimental fact that Ar′GeGeAr′ can react with up to 3 equiv of H_2 but Ar′SnSnAr′ reacts only with 1 equiv of H_2 is not due to higher reactivity of Ar′GeGeAr′ in comparison with Ar′SnSnAr′, as our mechanistic study found that Ar′GeGeAr′ has a slightly higher barrier than Ar′SnSnAr′. Ar′GeGeAr′ appears to be more reactive toward H_2 than Ar′SnSnAr′ is because of the greater ability of Ar′GeGeH$_2$Ar′ to undergo subsequent H_2 reductions. Similarly, because of the inert pair effect, the carbene-like Ar′HGe: species is able to activate H_2 while Ar′HSn: is inert toward H_2.

ASSOCIATED CONTENT

Supporting Information

Calibration of the DFT functional and basis set used (SI1 and SI2); optimized structures of stationary points shown in Scheme 2 (SI3); harmonic vibrational mode corresponding to the imaginary frrequency of transition state **TS1** (SI4); results of IRC calculations on the PhGeGePh model to verify the major steps involved in the mechanism (SI5−SI8); scanned potential energy surface for the association process Ar′HGe: +

dx.doi.org/10.1021/ja300111q | J. Am. Chem. Soc. 2012, 134, 8856−8868

Ar′HGe: → Ar′HGeGeHAr′ (SI9); optimized structures of stationary points labeled in Scheme 4 (SI10); harmonic vibrational mode corresponding to the imaginary frequency of transition state **TS13** (SI11); optimized structures of HGe(μ-H)GeH$_2$ at the TPSSTPSS, MP2, and CCSD(T)/BSI levels (SI12); scanned potential energy surface for the dissociation process Ar′HSnSnHAr′ → Ar′HSn: + Ar′HSn: (SI13); free energy profiles corresponding to Schemes 2 and 4 with scaled entropic contributions (SI14); optimized structures not shown in Figure 5 (SI15); optimized structures of Ar$^{\#}$Sn(μ-Cl)$_2$Ar$^{\#}$ and the Ar$^{\#}$ClSn: monomer (SI16); complete ref 26 (SI17); and total energies and Cartesian coordinates of all the structures involved in this study (SI18). This material is available free of charge via the Internet at http://pubs.acs.org.

AUTHOR INFORMATION

Corresponding Author

zxwang@gucas.ac.cn; schleyer@uga.edu

Notes

The authors declare no competing financial interest.

ACKNOWLEDGMENTS

This work was supported by the Chinese Academy of Sciences and the NSFC (Grants 20973197 and 21173263) and in the U.S. by NSF Grant CHE-1057466.

REFERENCES

(1) *Handbook of Homogeneous Hydrogenation*; de Vries, J. G., Elsevier, C. J., Eds.; Wiley-VCH: Weinheim, Germany, 2007.

(2) Kubas, G. J. *Metal Dihydrogen and σ-Bond Complexes*; Springer: New York, 2001.

(3) (a) Kubas, G. J. *Chem. Rev.* **2007**, *107*, 4152. (b) Kubas, G. J. *Science* **2006**, *314*, 1096. (c) Kubas, G. J. *Adv. Inorg. Chem.* **2004**, *56*, 127.

(4) Spikes, G. H.; Fettinger, J. C.; Power, P. P. *J. Am. Chem. Soc.* **2005**, *127*, 12232.

(5) (a) Himmel, H.-J. *Dalton Trans.* **2003**, 3639. (b) Himmel, H.-J.; Vollet, J. *Organometallics* **2002**, *21*, 5972. (c) Xiao, Z. L.; Hauge, R. H.; Margrave, J. L. *Inorg. Chem.* **1993**, *32*, 642.

(6) Berkessel, A.; Schubert, T. J. S.; Muller, T. N. *J. Am. Chem. Soc.* **2002**, *124*, 8693.

(7) Welch, G. C.; Juan, R. R. S.; Masuda, J. D.; Stephan, D. W. *Science* **2006**, *314*, 1124.

(8) (a) Stephan, D. W. *Org. Biomol. Chem.* **2008**, *6*, 1535 and references therein. (b) Stephan, D. W. *Dalton Trans.* **2009**, 3129 and references therein. (c) Stephan, D. W.; Erker, G. *Angew. Chem., Int. Ed.* **2010**, *49*, 46 and references therein. (d) Kenward, A. L.; Piers, W. E. *Angew. Chem., Int. Ed.* **2008**, *47*, 38 and references therein.

(9) (a) Rokob, T. A.; Hamza, A.; Stirling, A.; Soós, T.; Pápai, I. *Angew. Chem., Int. Ed.* **2008**, *47*, 2435.

(10) Guo, Y.; Li, S. H. *Inorg. Chem.* **2008**, *47*, 6212.

(11) (a) Wang, Z. X.; Lu, G.; Li, H. X.; Zhao, L. L. *Chin. Sci. Bull.* **2009**, *55*, 239. (b) Lu, G.; Li, H. X.; Zhao, L. L.; Huang, F.; Wang, Z. X. *Inorg. Chem.* **2010**, *49*, 295. (c) Lu, G.; Zhao, L. L.; Li, H. X.; Huang, F.; Wang, Z. X. *Eur. J. Inorg. Chem.* **2010**, 2254. (d) Lu, G.; Li, H. X.; Zhao, L. L.; Huang, F.; Schleyer, P. v. R.; Wang, Z. X. *Chem.—Eur. J.* **2011**, *17*, 2038.

(12) (a) Zhao, L. L.; Li, H. X.; Lu, G.; Wang, Z. X. *Dalton Trans.* **2010**, *39*, 4038. (b) Zhao, L. L.; Li, H. X.; Lu, G.; Huang, F.; Zhang, C. G.; Wang, Z. X. *Dalton Trans.* **2011**, *40*, 1929. (c) Li, H.; Zhao, L.; Lu, G.; Wang, Z.-X. *Dalton Trans.* **2010**, *39*, 5519. (d) Zhao, L. L.; Lu, G.; Huang, F.; Wang, Z. X. *Dalton Trans.* **2012**, *41*, 4674.

(13) Theuergarten, E.; Schluns, D.; Grunenberg, J.; Daniliuc, C. G.; Jones, P. G.; Tamm, M. *Chem. Commun.* **2010**, *46*, 8561.

(14) (a) Appelt, C.; Westenberg, H.; Bertini, F.; Ehlers, A. W.; Slootweg, J. C.; Lammertsma, K.; Uhl, W. *Angew. Chem., Int. Ed.* **2011**, *50*, 3925. (b) Bertini, F.; Lyaskovskyy, V.; Timmer, B. J. J.; de Kanter, F. J. J.; Lutz, M.; Ehlers, A. W.; Slootweg, J. C.; Lammertsma, K. *J. Am. Chem. Soc.* **2011**, *134*, 201.

(15) Frey, G. D.; Lavallo, V.; Donnadieu, B.; Schoeller, W. W.; Bertrand, G. *Science* **2007**, *316*, 439.

(16) (a) Senger, S.; Radom, L. *J. Phys. Chem. A* **2000**, *104*, 7375. (b) Senger, S.; Radom, L. *J. Am. Chem. Soc.* **2000**, *122*, 2613. (c) Chan, B.; Radom, L. *Aust. J. Chem.* **2004**, *57*, 659. (d) Chan, B.; Radom, L. *J. Am. Chem. Soc.* **2005**, *127*, 2443.

(17) (a) Chan, B.; Radom, L. *J. Am. Chem. Soc.* **2006**, *128*, 5322. (b) Chan, B.; Radom, L. *J. Am. Chem. Soc.* **2008**, *130*, 9790.

(18) For reviews, see: (a) Power, P. P. *Acc. Chem. Res.* **2011**, *44*, 627. (b) Power, P. P. *Nature* **2010**, *463*, 171. (c) Fischer, R. C.; Power, P. P. *Chem. Rev.* **2010**, *110*, 3877. (d) Power, P. P. *Appl. Organomet. Chem.* **2005**, *19*, 488. (e) Power, P. P. *Organometallics* **2007**, *26*, 4362. (f) Breher, F. *Coord. Chem. Rev.* **2007**, *251*, 1007. (g) Power, P. P. *Chem. Commun.* **2003**, 2091.

(19) For selected articles for Si and Pb, see: (a) Pu, L.; Twamley, B.; Power, P. P. *J. Am. Chem. Soc.* **2000**, *122*, 3524. (b) Sekiguchi, A.; Kinjo, R.; Ichinohe, M. *Science* **2004**, *305*, 1755. (c) Wiberg, N.; Vasisht, S. K.; Fischer, G.; Mayer, P. *Z. Anorg. Allg. Chem.* **2004**, *630*, 1823. (d) Kravchenko, V.; Kinjo, R.; Sekiguchi, A.; Ichinohe, M.; West, R.; Balazs, Y. S.; Schmidt, A.; Karni, M.; Apeloig, Y. *J. Am. Chem. Soc.* **2006**, *128*, 14472. (e) Kinjo, R.; Ichinohe, M.; Sekiguchi, A. *J. Am. Chem. Soc.* **2007**, *129*, 26. (f) Kinjo, R.; Ichinohe, M.; Sekiguchi, A.; Takagi, N.; Sumimoto, M.; Nagase, S. *J. Am. Chem. Soc.* **2007**, *129*, 7766. (g) Sekiguchi, A. *Pure Appl. Chem.* **2008**, *80*, 447. (h) Sasamori, T.; Hironaka, K.; Sugiyama, Y.; Takagi, N.; Nagase, S.; Hosoi, Y.; Furukawa, Y.; Tokitoh, N. *J. Am. Chem. Soc.* **2008**, *130*, 13856. (i) Han, J. S.; Sasamori, T.; Mizuhata, Y.; Tokitoh, N. *J. Am. Chem. Soc.* **2010**, *132*, 2546. (j) Takeuchi, K.; Ichinohe, M.; Sekiguchi, A. *J. Am. Chem. Soc.* **2008**, *130*, 16848. (k) Takeuchi, K.; Ichinohe, M.; Sekiguchi, A.; Guo, J. D.; Nagase, S. *Organometallics* **2009**, *28*, 2658. (l) Sasamori, T.; Han, J. S.; Hironaka, K.; Takagi, N.; Nagase, S.; Tokitoh, N. *Pure Appl. Chem.* **2010**, *82*, 603.

(20) For selected articles for Ge and Sn, see: (a) Stender, M.; Phillips, A. D.; Wright, R. J.; Power, P. P. *Angew. Chem., Int. Ed.* **2002**, *41*, 1785. (b) Phillips, A. D.; Wright, R. J.; Olmstead, M. M.; Power, P. P. *J. Am. Chem. Soc.* **2002**, *124*, 5930. (c) Spikes, G. H.; Peng, Y.; Fettinger, J. C.; Steiner, J.; Power, P. P. *Chem. Commun.* **2005**, 6041. (d) Peng, Y.; Fischer, R. C.; Merrill, W. A.; Fischer, J.; Pu, L.; Ellis, B. D.; Fettinger, J. C.; Herber, R. H.; Power, P. P. *Chem. Sci.* **2010**, *1*, 461. (e) Stender, M.; Phillips, A. D.; Power, P. P. *Chem. Commun.* **2002**, 1312. (f) Cui, C.; Olmstead, M. M.; Power, P. P. *J. Am. Chem. Soc.* **2004**, *126*, 5062. (g) Sugiyama, Y.; Sasamori, T.; Hosoi, Y.; Furukawa, Y.; Takagi, N.; Nagase, S.; Tokitoh, N. *J. Am. Chem. Soc.* **2006**, *128*, 1023. (h) Summerscales, O. T.; Jimenez-Halla, J. O. C.; Merino, G.; Power, P. P. *J. Am. Chem. Soc.* **2011**, *133*, 180. (i) Summerscales, O. T.; Fettinger, J. C.; Power, P. P. *J. Am. Chem. Soc.* **2011**, *133*, 11960. (j) Peng, Y.; Ellis, B. D.; Wang, X. P.; Fettinger, J. C.; Power, P. P. *Science* **2009**, *325*, 1668. (k) Summerscales, O. T.; Wang, X. P.; Power, P. P. *Angew. Chem., Int. Ed.* **2010**, *49*, 4788. (l) Spikes, G. H.; Power, P. P. *Chem. Commun.* **2007**, 85. (m) Wang, X. P.; Peng, Y.; Olmstead, M. M.; Fettinger, J. C.; Power, P. P. *J. Am. Chem. Soc.* **2009**, *131*, 14164. (n) Pu, L. H.; Phillips, A. D.; Richards, A. F.; Stender, M.; Simons, R. S.; Olmstead, M. M.; Power, P. P. *J. Am. Chem. Soc.* **2003**, *125*, 11626. (o) Fischer, R. C.; Pu, L.; Fettinger, J. C.; Brynda, M. A.; Power, P. P. *J. Am. Chem. Soc.* **2006**, *128*, 11366. (p) Peng, Y.; Ellis, B. D.; Wang, X.; Power, P. P. *J. Am. Chem. Soc.* **2008**, *130*, 12268. (q) Cui, C.; Brynda, M.; Olmstead, M. M.; Power, P. P. *J. Am. Chem. Soc.* **2004**, *126*, 6510. (r) Wang, X. P.; Zhu, Z. L.; Peng, Y.; Lei, H.; Fettinger, J. C.; Power, P. P. *J. Am. Chem. Soc.* **2009**, *131*, 6912. (s) Peng, Y.; Wang, X. P.; Fettinger, J. C.; Power, P. P. *Chem. Commun.* **2010**, *46*, 943. (t) Cui, C. M.; Olmstead, M. M.; Fettinger, J. C.; Spikes, G. H.; Power, P. P. *J. Am. Chem. Soc.* **2005**, *127*, 17530. (u) Rivard, E.; Steiner, J.; Fettinger, J. C.; Giuliani, J. R.; Augustine, M. P.; Power, P. P. *Chem. Commun.* **2007**, 4919.

(21) Peng, Y.; Brynda, M.; Ellis, B. D.; Fettinger, J. C.; Rivard, E.; Power, P. P. *Chem. Commun.* **2008**, 6042.

(22) (a) Zhu, Z. L.; Wang, X. P.; Peng, Y.; Lei, H.; Fettinger, J. C.; Rivard, E.; Power, P. P. *Angew. Chem., Int. Ed.* **2009**, *48*, 2031. (b) Fox, A. R.; Wright, R. J.; Rivard, E.; Power, P. P. *Angew. Chem., Int. Ed.* **2005**, *44*, 7729. (c) Hardman, N. J.; Wright, R. J.; Phillips, A. D.; Power, P. P. *J. Am. Chem. Soc.* **2003**, *125*, 2667. (d) Zhu, Z. L.; Wang, X. P.; Olmstead, M. M.; Power, P. P. *Angew. Chem., Int. Ed.* **2009**, *48*, 2027. (e) Zhu, Z. L.; Wright, R. J.; Brown, Z. D.; Fox, A. R.; Phillips, A. D.; Richards, A. F.; Olmstead, M. M.; Power, P. P. *Organometallics* **2009**, *28*, 2512.

(23) Li, J.; Schenk, C.; Goedecke, C.; Frenking, G.; Jones, C. *J. Am. Chem. Soc.* **2011**, *133*, 18622.

(24) (a) Chen, Y.; Hartmann, M.; Diedenhofen, M.; Frenking, G. *Angew. Chem., Int. Ed.* **2001**, *40*, 2052. (b) Lein, M.; Krapp, A.; Frenking, G. *J. Am. Chem. Soc.* **2005**, *127*, 6290. (c) Kobayashi, K.; Nagase, S. *Organometallics* **1997**, *16*, 2489. (d) Nagase, S.; Kobayashi, K.; Takagi, N. *J. Organomet. Chem.* **2000**, *611*, 264. (e) Kobayashi, K.; Takagi, N.; Nagase, S. *Organometallics* **2001**, *20*, 234. (f) Takagi, N.; Nagase, S. *Organometallics* **2001**, *20*, 5498. (g) Takagi, N.; Schmidt, M. W.; Nagase, S. *Organometallics* **2001**, *20*, 1646. (h) Takagi, N.; Nagase, S. *Eur. J. Inorg. Chem.* **2002**, 2775. (i) Takagi, N.; Nagase, S. *Organometallics* **2007**, *26*, 469. (j) Rivard, E.; Fischer, R. C.; Wolf, R.; Peng, Y.; Merrill, W. A.; Schley, N. D.; Zhu, Z. L.; Pu, L.; Fettinger, J. C.; Teat, S. J.; Nowik, I.; Herber, R. H.; Takagi, N.; Nagase, S.; Power, P. P. *J. Am. Chem. Soc.* **2007**, *129*, 16197. (k) Jung, Y.; Brynda, M.; Power, P. P.; Head-Gordon, M. *J. Am. Chem. Soc.* **2006**, *128*, 7185. (l) Takagi, N.; Nagase, S. *Organometallics* **2007**, *26*, 3627.

(25) Peng, Y.; Guo, J. D.; Ellis, B. D.; Zhu, Z. L.; Fettinger, J. C.; Nagase, S.; Power, P. P. *J. Am. Chem. Soc.* **2009**, *131*, 16272.

(26) Frisch, M. J.; et al. *Gaussian 03*, revision E.01; Gaussian, Inc.: Wallingford, CT, 2004.

(27) (a) Heyd, J.; Scuseria, G. E. *J. Chem. Phys.* **2004**, *121*, 1187. (b) Boese, A. D.; Klopper, W.; Martin, J. M. L. *Int. J. Quantum Chem.* **2005**, *104*, 830. (c) Sonk, J. A.; Schlegel, H. B. *J. Phys. Chem. A* **2011**, *115*, 11832.

(28) (a) Becke, A. D. *Phys. Rev. A* **1988**, *38*, 3098. (b) Perdew, J. P.; Wang, Y. *Phys. Rev. B* **1992**, *45*, 13244.

(29) (a) Lee, C. T.; Yang, W. T.; Parr, R. G. *Phys. Rev. B* **1988**, *37*, 785. (b) Becke, A. D. *J. Chem. Phys.* **1993**, *98*, 5648.

(30) (a) Zhao, Y.; Schultz, N. E.; Truhlar, D. G. *J. Chem. Theory Comput.* **2006**, *2*, 364. (b) Zhao, Y.; Truhlar, D. G. *Acc. Chem. Res.* **2008**, *41*, 157.

(31) (a) Fuentealba, P.; Preuss, H.; Stoll, H.; Vonszentpaly, L. *Chem. Phys. Lett.* **1982**, *89*, 418. (b) Vonszentpaly, L.; Fuentealba, P.; Preuss, H.; Stoll, H. *Chem. Phys. Lett.* **1982**, *93*, 555. (c) Fuentealba, P.; Stoll, H.; Vonszentpaly, L.; Schwerdtfeger, P.; Preuss, H. *J. Phys. B* **1983**, *16*, L323.

(32) (a) Hay, P. J.; Wadt, W. R. *J. Chem. Phys.* **1985**, *82*, 270. (b) Hay, P. J.; Wadt, W. R. *J. Chem. Phys.* **1985**, *82*, 299. (c) Wadt, W. R.; Hay, P. J. *J. Chem. Phys.* **1985**, *82*, 284.

(33) Peterson, K. A. *J. Chem. Phys.* **2003**, *119*, 11099.

(34) Weigend, F.; Ahlrichs, R. *Phys. Chem. Chem. Phys.* **2005**, *7*, 3297.

(35) Francl, M. M.; Pietro, W. J.; Hehre, W. J.; Binkley, J. S.; Gordon, M. S.; Defrees, D. J.; Pople, J. A. *J. Chem. Phys.* **1982**, *77*, 3654.

(36) (a) Li, Y. F.; Zhu, J. Q.; Liu, H.; He, P.; Wang, P.; Tian, H. P. *Bull. Korean Chem. Soc.* **2011**, *32*, 1851. (b) Lomratsiri, J.; Probst, M.; Limtrakul, J. *J. Mol. Graphics* **2006**, *25*, 219. (c) Namuangruk, S.; Khongpracha, P.; Pantu, P.; Limtrakul, J. *J. Phys. Chem. B* **2006**, *110*, 25950.

(37) (a) Mennucci, B.; Tomasi, J. *J. Chem. Phys.* **1997**, *107*, 3032. (b) Mennucci, B.; Tomasi, J. *J. Chem. Phys.* **1997**, *106*, 5151. (c) Mennucci, B.; Cancès, E.; Tomasi, J. *J. Phys. Chem. B* **1997**, *101*, 10506. (d) Tomasi, J.; Mennucci, B.; Cancès, E. *J. Mol. Struct.* **1999**, *464*, 211.

(38) Rappe, A. K.; Casewit, C. J.; Colwell, K. S.; Goddard, W. A., III; Skiff, W. M. *J. Am. Chem. Soc.* **1992**, *114*, 10024.

(39) Grützmacher, H. *Angew. Chem., Int. Ed.* **2008**, *47*, 1814.

(40) Geier, S. J.; Gilbert, T. M.; Stephan, D. W. *J. Am. Chem. Soc.* **2008**, *130*, 12632.

(41) Richards, A. F.; Phillips, A. D.; Olmstead, M. M.; Power, P. P. *J. Am. Chem. Soc.* **2003**, *125*, 3204.

(42) Eichler, B. E.; Pu, L. H.; Stender, M.; Power, P. P. *Polyhedron* **2001**, *20*, 551.

(43) (a) Trinquier, G. *J. Am. Chem. Soc.* **1991**, *113*, 144. (b) Treboux, G.; Trinquier, G. *Inorg. Chem.* **1992**, *31*, 4201. (c) Trinquier, G. *J. Chem. Soc., Faraday Trans.* **1993**, *89*, 775.

(44) (a) Hermans, J.; Wang, L. *J. Am. Chem. Soc.* **1997**, *119*, 2707. (b) Strajbl, M.; Sham, Y. Y.; Villà, J.; Chu, Z. T.; Warshel, A. *J. Phys. Chem. B* **2000**, *104*, 4578. (c) Yu, Z.-X.; Houk, K. N. *J. Am. Chem. Soc.* **2003**, *125*, 13825. (d) Chen, Y.; Ye, S.; Jiao, L.; Liang, Y.; Sinha-Mahapatra, D. K.; Herndon, J. W.; Yu, Z. X. *J. Am. Chem. Soc.* **2007**, *129*, 10773. (e) Liang, Y.; Liu, S.; Xia, Y. Z.; Li, Y. H.; Yu, Z. X. *Chem.—Eur. J.* **2008**, *14*, 4361. (f) Liang, Y.; Liu, S.; Yu, Z. X. *Synlett* **2009**, 905.

(45) (a) Bennaim, A.; Marcus, Y. *J. Chem. Phys.* **1984**, *81*, 2016. (b) Tissandier, M. D.; Cowen, K. A.; Feng, W. Y.; Gundlach, E.; Cohen, M. H.; Earhart, A. D.; Coe, J. V.; Tuttle, T. R. *J. Phys. Chem. A* **1998**, *102*, 7787. (c) Kelly, C. P.; Cramer, C. J.; Truhlar, D. G. *J. Phys. Chem. B* **2006**, *110*, 16066.

(46) According to Wikipedia, "The inert pair effect is the tendency of the outermost s electrons to remain unionized or unshared in compounds of post-transition metals. The term **inert pair effect** is often used in relation to the increasing stability of oxidation states that are 2 less than the group valency for the heavier elements of groups 13, 14, 15, and 16. The term 'inert pair' was first proposed by Nevil Sidgwick in 1927." For details, see: (a) http://en.wikipedia.org/wiki/Inert_pair_effect. (b) Sidgwick, N. V. *The Electronic Theory of Valency*; Clarendon Press: Oxford, U.K., 1927; p 178. (c) Sidgwick, N. V. *The Chemical Elements and Their Compounds*; Clarendon Press; Oxford, U.K., 1950; p 287.